HHS Public Access

Author manuscript

J Alzheimers Dis. Author manuscript; available in PMC 2021 May 15.

Published in final edited form as:

J Alzheimers Dis. 2021 ; 79(3): 1235–1255. doi:10.3233/JAD-201099.

Gut Inflammation Induced by Dextran Sulfate Sodium Exacerbates Aβ Plaque Deposition in the *App*$^{NL\text{-}G\text{-}F}$ Mouse Model of Alzheimer's Disease

Mona Sohrabi,

Department of Biomedical Sciences, University of North Dakota School of Medicine & Health Sciences, Grand Forks, ND

Heidi L. Pecoraro,

Veterinary Diagnostic Laboratory, North Dakota State University, Fargo ND

Colin K. Combs*

Department of Biomedical Sciences, University of North Dakota School of Medicine & Health Sciences, Grand Forks, ND

Abstract

Background: Although it is known that the brain communicates with the gastrointestinal (GI) tract via the well-established gut-brain axis, the influence exerted by chronic intestinal inflammation on brain changes in Alzheimer's disease (AD) is not fully understood. We hypothesized that increased gut inflammation would alter brain pathology of a mouse model of AD.

Methods: To test this idea, 2% dextran sulfate sodium (DSS) was dissolved in the drinking water and fed *ad libitum* to male C57BL/6 wild type and *App*$^{NL\text{-}G\text{-}F}$ mice at 6–10 months of age for two cycles of three days each. DSS is a negatively charged sulfated polysaccharide which results in bloody diarrhea and weight loss, changes similar to human inflammatory bowel disease (IBD).

Results: Both wild type and *App*$^{NL\text{-}G\text{-}F}$ mice developed an IBD-like condition. Brain histologic and biochemical assessments demonstrated increased insoluble $A\beta_{1–40/42}$ levels along with the decreased microglial CD68 immunoreactivity in DSS treated *App*$^{NL\text{-}G\text{-}F}$ mice compared to vehicle treated *App*$^{NL\text{-}G\text{-}F}$ mice.

Conclusions: These data demonstrate that intestinal dysfunction is capable of altering plaque deposition and glial immunoreactivity in the brain. This study increases our knowledge of the impact of peripheral inflammation on Aβ deposition via an IBD-like model system.

Keywords

Alzheimer's disease; Neuroinflammation; Aβ deposition; Dextran sulfate sodium; Inflammatory bowel disease

***Correspondence Address**: 1301 North Columbia Road, Stop 9037, Department of Biomedical Sciences, University of North Dakota School of Medicine & Health Sciences, Grand Forks, ND 58202-9037, phone 701-777-4025, colin.combs@med.und.edu.

CONFLICT OF INTEREST/DISCLOSURE STATEMENT

The authors have no conflict of interest to report.

INTRODUCTION

Alzheimer's disease (AD) is a progressive age-related neurodegenerative disorder and the most common form of dementia [1]. The disease is characterized by the accumulation of extracellular Aβ plaque deposition, intracellular neurofibrillary tangles, and neuroinflammation, including microgliosis and astrocytosis [2–6]. These pathophysiological features spread throughout brain regions as the disease progresses and result in neuronal death, synaptic loss, and learning and memory decline [1, 7–11]. Neuroinflammation plays a pivotal role in the susceptibility, onset, and progression of AD [12, 13]. Numerous retrospective studies demonstrate a significant reduction in the risk of AD in correlation with prolonged use of non-steroidal anti-inflammatory drugs (NSAIDs) early in life [14–17]. A midlife elevation of inflammatory markers due to systemic inflammation was also associated with increased cognitive decline over the course of 20 years in older adulthood in a longitudinal human study [18]. Observational studies demonstrate that individuals with one or more major infections, including *pneumonia*, during midlife or later adulthood have higher risk of diminished brain volumes, dementia, and AD pathology hallmarks [19].

In addition to the central nervous system being affected by age, elderly frequently suffer from gastrointestinal inflammation and dysfunction, including fecal incontinence, constipation, microscopic colitis, and diarrhea [20–25]. Indeed, inflammatory bowel disease (IBD), including colitis and Crohn's disease, is associated with risk of developing AD, cognitive impairment, anxiety, and depression in patients [26–32]. This relationship may be due to the fact that the gastrointestinal (GI) tract bi-directionally communicates with the brain via the well-established gut-brain axis, including direct neuronal communication, endocrine signaling markers, and the immune system [33]. In our prior work we have shown intestinal changes in both human AD and mouse models that correlate with changes in the brains supporting the notion that brain and intestinal changes may be linked during disease [34, 35]. The human GI tract harbors 100 trillion microbes, 10 times more than the human body total cells, which mostly reside in the colon and play a critical role in regulating intestinal function [36]. Intestinal dysbiosis, changes in intestinal microbial diversity, have been reported in both human and animal models of IBD [37–44] and Alzheimer's disease alike [45–47] again suggesting a gut-brain connection during disease. Most importantly, intestinal inflammation in IBD mouse models results in microglial activation, altered neurogenesis, and increased cortical inflammation [48–50]. The complex gut brain communication mechanisms disrupted during colitis may influence brain function in numerous fashions involving changes in the innate and acquired immune system, the autonomic and enteric nervous systems, the endocrine system, the hypothalamic-pituitary-adrenal axis, and even intestinal microbial products and metabolites [51–65]. For example, one well described gut brain communication mechanism that is particularly relevant to intestinal inflammation involves damage to the epithelium which may allow leakage of bacteria or bacterial products such as LPS into the tissue parenchyma to stimulate systemic inflammation associated with elevations of cytokines such as TNFα and IL-6 which are well known to influence and correlate with behavior changes [51–54, 66–72].

In this study, we tested the hypothesis that induction of moderate colonic inflammation potentiates the progression of AD propagated from the intestine to the brain. Wild type and $App^{NL\text{-}G\text{-}F}$ mice were orally treated with 2 cycles of 2% dextran sulfate sodium (DSS) for 3 days followed by 14 days of interval. Mice were assessed for changes in memory and anxiety-like behavior during the second recovery phase and sacrificed 20 days after the last DSS exposure to investigate the long-lasting impact of gut inflammation on AD mouse brains. Our data demonstrated that chronic DSS administration decreased locomotion activity but not memory function and increased Aβ plaque load correlating with decreased microglial phagocytic phenotype in the AD mouse model.

MATERIALS AND METHODS

Animal models

$App^{NL\text{-}G\text{-}F}$ mice (KI:RBRC06344) were obtained from Dr. Takashi Saito and Dr. Takaomi C. Saido, RIKEN BioResource Center, Japan. These mice carry the humanized Aβ region, including Swedish (NL), Arctic (G), and Beyreuther/Iberian (F) mutations which promotes Aβ production, enhances Aβ aggregation through facilitating oligomerization and reducing proteolytic degradation, and increases $Aβ_{42/40}$ ratio, respectively [73]. This transgenic mouse model of AD develops cortical Aβ amyloidosis as early as 2 months. To perform this study, wild-type (WT) C57BL/6 mice originally purchased from the Jackson Laboratory (Bar Harbor, Maine) and the $App^{NL\text{-}G\text{-}F}$ transgenic mice were maintained, as a colony, under standard housing conditions including a 12 h light:12 h dark cycle and 22 ± 1°C temperature with *ad libitum* access to food and water at the University of North Dakota Center for Biomedical Research. Male C57BL/6 control WT and $App^{NL\text{-}G\text{-}F}$ mice at 6–10 months of age (n = 9–11 per treatment group) were used (Table 1). Although sex differences are important to consider, particularly in the AD field, for this study we did not have adequate numbers of female mice at the onset of the study due to breeding needs and other experimental uses and we elected to proceed with a male only study with the rationale that males are more susceptible to inflammation induced by DSS and develop severe and aggressive disease [74]. Mice were randomly divided into vehicle and DSS treated groups for 8 weeks of investigation. Mice were euthanized followed by cardiac perfusion and the brain, spleen, and colon were collected to quantify histologic and biochemical changes on week 8. All procedures involving animals were reviewed and approved by the UND Institutional Animal Care and Use Committee (UND IACUC). The investigation conforms to the National Research Council of the National Academies Guide for the Care and Use of Laboratory Animals (8^{th} edition).

DSS exposure and assessment of the severity of colitis-like symptoms

To mimic the effect of gut inflammation on the progression of AD in adulthood, 6–10 months-old male $App^{NL\text{-}G\text{-}F}$ mice and matched sex WT mice were randomly divided into 4 experimental groups (Table 1). As evaluating the role of peripheral inflammation on AD brain effects during adulthood was the goal of the study, we elected to study mice at an older age (approximately 10 month of age for AD mice and 7 month of age for the WT groups). Each genotype was treated with vehicle (autoclaved drinking water) or 2% DSS for 2 cycles, 3 days each, with 14 days of interval for recovery before initiation of the second DSS

exposure as described in Fig. 1 [75]. Colitis-like disease was induced in two groups by dissolving DSS (2%, w/v, MW=36–50 kDa, MP Biomedicals, LLC, Santa Ana, CA, USA) in autoclaved drinking water. Mice were weighed individually on day 0, every day during the second cycle of the DSS treatment, 2 days post exposure, and twice a week to the end of the study (Supplementary Table 1). Drinking water as well as food intake in each cage were monitored every day during the DSS bouts and weekly throughout the rest of the experimental procedure without making specific measurements but to ensure consumption was occurring. The disease activity index (DAI) is associated with the presence of gut lesions and inflammation and represents the percentage of body weight loss, stool consistency, and the presence of gross bleeding in feces. A Hemoccult test kit (Beckman Coulter Inc., CA, USA) was used to determine occult blood in the stool samples. DAI was evaluated and scored in a blinded fashion at 1 day prior to DSS treatment (day 0), during the second cycle of 2% DSS administration, and 2 days post exposure, totaling 5 days, as previously described with slight modifications (Table 2) [76–80]. Each parameter was scored on a scale of 0–4 and summed to get a score out of 12 for the maximum DAI per mouse for each condition. The daily DAI per mouse was subtracted from its respective day 0 to get the normalized score. Body weight loss was calculated as the percentage ratio by dividing the body weight on each specific day by the body weight on day 0 during the second cycle of 2% DSS administration until the week of mice collection (Fig. 1). The method of scoring is quite analogous to clinical symptoms observed in human IBD. Mice were approximately 8–12 months of age at the time of collection. On the 8^{th} week, animals were euthanized via CO_2 asphyxiation followed by cardiac exsanguination and perfusion with PBS. The colon weights and lengths between the cecum and rectum as well as spleen weights were measured post-mortem. The brain, colon, and spleen were collected for further histochemical and biochemical analysis.

Histological staining and scoring of colonic tissue

On the day of collection, distal colons were made into Swiss rolls, fixed in 4% paraformaldehyde (PFA) for 5 days, and cryoprotected via two successive changes of 30% sucrose. The Swiss-rolls were embedded into gelatin blocks and were serially sectioned using a chambered cryostat for 10μm thick sections. Colon sections were stained for histology H&E (Hematoxylin and eosin) and Alcian blue stains as described in detail previously [81]. H&E sections were examined by a pathologist blinded to the experimental groups. Histological scoring was assigned based on the extent of inflammation and mucosal hyperplasia as follow A) inflammation score: 0= normal (within normal limits); 1= mild (small, focal, or widely separated, limited to lamina propria); 2= moderate (multifocal or locally extensive, extending to submucosa); 3= severe (transmural inflammation) and B) mucosal hyperplasia score: 0= normal (within normal limits); 1= mild (crypts 2–3 times normal thickness, normal epithelium); 2= moderate (crypts 2–3 times normal thickness, hyperchromatic epithelium, reduced goblet cells, scattered arborization); 3= severe (crypts ≥ 4 times normal thickness, marked hyperchromasia, few to no goblet cells, high mitotic index, frequent arborization) [82]. Individual and sum of two histology scores were graphed for better data interpretation. The stained slides were scanned using a Hamamatsu 2.0HT digital slide scanner and figures were made using Adobe Photoshop CS3 software (Adobe Systems, San Jose, CA). Colonic images are shown with 10X and 20X magnifications.

Behavioral analysis: Open field and Cross-Maze tests

On the 7th week, open field (OF) and cross maze (CM) tests were performed to assess the effect of DSS treatment on behavior during the second recovery phase. Locomotor activity and working memory were evaluated by OF and CM tests, respectively. To evaluate general locomotion associated with treatment, animals were placed individually in the same quadrant of a 19cm × 45cm × 25cm open field apparatus to freely explore and move for 10 min. The distance traveled, time spent in the center of the field as well as time mobile were scored blindly from video captured by Anymaze software (Stoelting Co. Wood Dale, IL, USA). Following the test, the animals were placed back into their home cages for at least 30 min prior to the next behavior assessment.

CM testing allows mice to explore a cross-shaped maze at their own discretion without any added stress or motivation such as lights, sound, food deprivation, etc. Mice were placed in the same arm of the CM and allowed to move and choose other arms for 10 min. A choice was considered when all 4 feet were within an arm. The total entries (the total number of choices made by each animal) were recorded and the number of alternations was counted (defined as 4 consecutive entries into 4 different arms), and % alternation for each mouse was calculated as follows, # alternations/(total entries-3) x 100, blindly from video captured using Anymaze software (Stoelting Co. Wood Dale, IL, USA). Immediate re-entry into the same arm, after exiting it, was not considered as an arm choice. The chance alternation rate for this task is 22.2%. After completion of the test, mice were returned to their home cages until tissue collection.

Immunohistochemistry (IHC)

Left brain hemispheres were fixed in 4% PFA for 5 days followed by cryoprotection via two successive changes of 30% sucrose. Brains were embedded in 15% gelatin and serially sectioned into 40μm sections using a sliding microtome [83]. Sections were immunostained using antibodies against Iba-1 (1:1000 dilution, rabbit, 019–19741, Wako Chemicals USA, Inc., Richmond, VA, USA), CD68 (1:1000 dilution, rat anti-mouse, MCA1957, Bio-Rad Laboratories, Inc., CA, USA), GFAP (1:1000 dilution, D1F4Q, rabbit mAb, Cell Signaling Technology, Inc., Danvers, MA, USA), and Aβ (1:500 dilution, D54D2, rabbit mAb, human cross-reactivity, Cell Signaling Technology, Inc., Danvers, MA, USA) to detect microglia, astrocytes, and Aβ plaques, respectively. For Aβ immunostaining, antigen retrieval was required and performed using 25% formic acid (Sigma-Aldrich) for 25 min at room temperature prior to blocking (Burlingame, CA, USA). Immunostaining was performed for the Swiss-rolls via using rat anti-mouse CD68 (1:1000 dilution, MCA1957, Bio-Rad Laboratories, Inc., CA, USA) antibody to target the intestinal macrophages [81]. Tissues were rinsed in PBS and blocked in PBS solution containing 0.5% bovine serum albumin (BSA, Equitech-Bio, Inc.), 0.1% Triton X-100 (Sigma-Aldrich), 5% normal goat serum (NGS, Equitech-Bio, Inc.), and 0.02% Na Azide for at least 30 min. After 24 hr of incubating tissues with primary antibodies at 4°C, respective biotinylated secondary antibodies were used, including rabbit anti-rat IgG antibody mouse adsorbed and goat anti-rabbit IgG (Vector Laboratories, Inc., Burlingame, CA, USA). A VECTASTAIN Avidin-Biotin Complex (ABC) kit was used followed by the Vector VIP Peroxidase (HRP) Substrate kit (SK-4600) to visualize the antibody binding (Vector laboratories, Inc.,

Burlingame, CA, USA). For analysis and quantitation, images were taken using an upright Leica DM1000 microscope and Leica DF320 digital camera. Immunohistochemistry quantitation was performed using 3 serial sections containing either hippocampi or temporal cortices per mouse (n=5–9). A total of 4 distal colonic Swiss-rolls per condition were quantified for CD68 immunohistochemistry. The images were converted into greyscale followed by inversion using Adobe Photoshop CS3 software (Adobe Systems, San Jose, CA). After normalizing background, the mean optical density value for each image was recorded by selecting the whole hippocampus, temporal cortex, or Swiss-roll using the lasso tool in Adobe Photoshop CS3 software (Adobe Systems, San Jose, CA) and interested areas selected using a WACOM tablet model: CTE-430 (WACOM Co., Ltd). Brain (4X and 20X magnifications) and colonic (10X and 20X magnifications) images were taken via a Hamamatsu 2.0HT digital slide scanner.

Enzyme-linked immunosorbent assay (ELISA)

On the collection day, right hippocampi and parietal cortices of brain hemispheres and middle parts of the colons were isolated and flash frozen. Hippocampi, parietal cortices, and middle colons were lysed in RIPA buffer (20 mM Tris, pH 7.4, 150 mM NaCl, 1 mM $Na3VO_4$, 10 mM NaF, 1 mM EDTA, 1 mM EGTA, 0.2 mM phenylmethylsulfonyl fluoride, 1% Triton X-100, 0.1% SDS, and 0.5% deoxycholate), lysis buffer 17 (R&D Systems, a Bio-techne brand, Minneapolis, MN, USA), and 1% Triton X-100 in PBS, respectively, with protease inhibitor cocktail (P8340, Sigma-Aldrich, MO, USA). Tissues were centrifuged (12,000 rpm, 4°C, 10 min) and the supernatants were collected. Hippocampi supernatants were used to perform soluble $A\beta_{1-40/42}$ ELISAs (human Amyloid $\beta_{40/42}$ Brain EZBRAIN40/42 ELISA, EMD Millipore, Billerica, MA, USA). The hippocampi pellets were re-suspended in 5M guanidine HCL/50mM Tris HCL, pH 8.0, centrifuged (12,000 rpm, 4°C, 10 min), and the supernatants were removed to quantify insoluble $A\beta_{1-40/42}$ levels by using the same ELISA kit according to the manufacturer's protocol. TNF-α, IL-1β, and IL-6 cytokine ELISAs were performed from the parietal cortices supernatants according to the manufacturer's protocol (Quantikine ELISAs, R&D Systems, a bio-techne brand, Minneapolis, MN, USA). The collected colon supernatants were used to perform lipocalin-2 ELISA (Mouse Lipocalin-2/NGAL DuoSet ELISA, R&D Systems, a bio-techne brand, Minneapolis, MN, USA) according to the manufacturer's protocol. The BCA kit (Thermo Scientific, IL, USA) were used to quantify protein concentrations and Aβ, lipocalin-2, and cytokine levels were normalized to the protein content of each homogenized sample.

Western blotting

Protein contents were assessed for the collected hippocampi supernatants, previously lysed in RIPA buffer containing protease inhibitor cocktail, via a BCA kit. Five μg of protein per sample was resolved by 10% sodium dodecyl sulfate polyacrylamide gel electrophoresis (SDS-PAGE) and transferred to polyvinylidene difluoride membranes (PVDF) for western blotting. Membranes were blocked for 1h in 5% bovine serum albumin (BSA) in tris-buffered saline solution (TBST) followed by applying anti-amyloid precursor protein (1:1000 dilution, Y188, ab32136, rabbit mAb, mouse/rat/human cross-reactivity, Abcam, Cambridge, MA, USA), BACE (1:1000 dilution, D10E5, rabbit mAb, Cell Signaling Technology, Inc., Danvers, MA, USA), and Cox-2 (1:500 dilution, Cyclooxygenase 2, rabbit

pAb, ab15191, Abcam, Cambridge, MA, USA), primary antibodies overnight at 4°C. Chemiluminescent visualization was used to detect antibody binding using donkey anti-rabbit IgG and goat-anti mouse IgM horseradish peroxidase (HRP)-conjugated secondary antibodies (Santa Cruz Biotechnology, Inc., CA, USA). Exposures were captured using an Aplegen Omega Lum G imaging system. Optical density values were normalized to the loading control α-tubulin (1:10000 dilution, TU-02: sc-8035, mouse mAb, Santa Cruz Biotechnology, Inc., CA, USA) optical density values.

Statistical analysis

All *in vivo* data, except DAI and %BW changes, were analyzed by performing unpaired two-tailed t-test. DAI and %BW changes were analyzed via two-way ANOVA multiple comparisons followed by uncorrected Fisher's LSD test using GraphPad Prism 8 software. Data are represented as the mean ± SEM. Significance is indicated by P value measurements with a $P < 0.05$ considered significant; *$P < 0.05$; **$P < 0.01$; ***$P < 0.001$; ****$P < 0.0001$.

RESULTS

DSS induced colitis-like symptoms in wild type and *App*$^{NL-G-F}$ mice

Six-ten months-old male *App*$^{NL-G-F}$ mice and matched sex WT mice (Table 1) were treated with 2% DSS for 2 bouts to induce colonic inflammation. Symptomatic parameters of colitis, DAI (Table 2) and % body weight loss, were monitored and recorded during the experimental procedure as indicated in Fig. 1. Colon length as well as spleen and colon weights were measured postmortem on the day of tissue collection. During the second administration of DSS, both WT and AD mouse models displayed significantly greater disease activity scores and % body weight losses compared to their respective untreated groups starting on days 1 and 4, respectively (Fig. 2A-D). Mice were expected to recover to their initial weight during the course of recovery [80]. However, both WT and *App*$^{NL-G-F}$ DSS treated mice showed a consistent reduction in body weight and without complete recovery after ending the second cycle of DSS exposure until euthanasia in comparison with their controls (Fig. 2C and D). Body weight loss and rectal bleeding are associated with shortening and thickening of the colon as well as splenomegaly, as other biological markers for assessment of colonic inflammation [76, 84]. The 2% chronic DSS treated group in both genotypes demonstrated a significant increase in spleen and colon weights typically related to anemia as a result of rectal bleeding [84] and the granulomatous nature of inflammation [76], respectively (Fig. 2E and F). Colonic length significantly decreased in WT, but not *App*$^{NL-G-F}$ mice as expected after inflammatory induction perhaps indicating a less severe response to DSS in *App*$^{NL-G-F}$ mice (Fig. 2G). Overall, these results demonstrated that 2 cycles of chronic DSS treatment produced a time-dependent DAI in both WT and *App*$^{NL-G-F}$ genotypes.

DSS administration disrupted colonic epithelial integrity and increased inflammation

In order to perform histological examination of colonic inflammation induced by DSS, H&E and Alcian blue staining were performed on the distal colon Swiss-rolls (Fig. 3). Hematoxylin and eosin staining examination demonstrated significantly greater

inflammation (severe) (Fig. 3C), mucosal hyperplasia (mild for WT and moderate for App^{NL-G-F}) (Fig. 3D), and total histology lesions (Fig. 3E) in DSS treated WT and App^{NL-G-F} mice compared to their respective controls. To better assess goblet cell loss caused by chronic DSS exposure, mucin-producing goblet cells were visualized by performing Alcian blue staining. Alcian blue stains acidic mucus secreted by goblet cells [85]. Alcian blue staining frequently highlighted goblet cells lining crypts of the control vehicle groups. However, crypt epithelial cells only occasionally stained with Alcian blue in areas of hyperplasia in the WT and App^{NL-G-F} DSS treated groups. Also, fewer goblet cells in regions of inflammation with mucosal erosion were observed as a result of DSS treatment (Fig. 3B). Briefly, the number of goblet cells markedly decreased within areas of mucosal hyperplasia and inflammation due to DSS treatment compared to the respective vehicle groups in both genotypes (Fig. 3B). It has been reported that the number of CD68 positive macrophages increases in colon specimens of IBD patients compared to normal individuals [86]. Therefore, CD68 immunostaining was performed to visualize infiltrating, activated macrophages, into the lamina propria and colonic submucosa. As expected, a robust and statistically significant increase in macrophage infiltration to the site of inflammation was observed in both DSS treated genotypes in comparison with controls (Fig. 4A and B). Lipocalin-2 (Lcn2), as a 25 kDa neutrophil gelatinase-associated lipocalin (NGAL) glycoprotein, was first isolated from human neutrophil granules [87]. Fecal Lcn2 is a stable, highly sensitive, and non-invasive marker which determines the extent of intestinal inflammation [84]. Colonic lipocalin ELISA demonstrated a significant increase in response to DSS treatment in App^{NL-G-F} and WT mice compared to their controls (Fig. 4C). Although lipocalin is only one biomarker of colonic inflammation, an apparent slightly greater DSS-induced increase in WT compared to App^{NL-G-F} mice suggests that the colonic response may be less severe in the AD line. These findings suggest that 2% chronic DSS administration induced moderate expression of inflammatory markers in both genotypes.

DSS treatment decreased mobility of App^{NL-G-F} mice

To determine whether induction of moderate colonic inflammation negatively affects locomotor activity and working memory, WT and App^{NL-G-F} mice were examined in the OF and CM paradigms 12 days after completing the second cycle of DSS, during the resolving inflammation/recovery phase. The OF test examines general locomotion and anxiety-like behavior via primarily exploratory behavior [88]. Comparing only within genotype, mobility as well as time mobile were significantly attenuated due to DSS administration in the App^{NL-G-F} mice. However, DSS exposure exerted no effect on time spent in the center of the OF in either genotypes (Fig. 5A). Surprisingly, although the WT mice demonstrated biochemical and histologic evidence of colonic inflammation it may not have been sufficient to produce robust behavioral differences detectable with the open field test we elected to use [89]. This suggests a basal increase in locomotion activity was present in App^{NL-G-F} mice which was attenuated by DSS treatment.

To assess the working memory changes induced by 2 bouts of 2% DSS treatment, performance in the CM paradigm, which is a “+” shaped apparatus with four white arms, was examined for both genotypes [90]. Consistent with the OF results, the total number of arm choices (total entries: locomotor activity indicator), which was greater in vehicle treated

$App^{NL\text{-}G\text{-}F}$, significantly reduced in AD mice after DSS administration (Fig. 5B). There was no significant decrease in % alternations (indicator of memory deficit) due to DSS treatment in either genotypes (Fig. 5B). Like the mobility findings, it is unclear why the DSS-induced colonic inflammation did not produce memory deficits. It is possible that changes were simply not detectable with the CM test or even greater inflammatory insult is required to affect behavior. Collectively, DSS exposure negatively affected $App^{NL\text{-}G\text{-}F}$ mice locomotion during the second recovery phase.

Gut inflammation induced by DSS altered Aβ accumulation in $App^{NL\text{-}G\text{-}F}$ mice brains

WT and $App^{NL\text{-}G\text{-}F}$ mice were treated with 2 cycles of 2% DSS and sacrificed 20 days (on week 8^{th}) after the last exposure (Fig. 1) to assess long-lasting brain changes. The impact of moderate disruption of gut epithelial barrier and gut inflammation on Aβ deposition in different brain regions was assessed. Aβ immunohistochemistry demonstrated that plaque load significantly increased in both hippocampi and temporal cortices of $App^{NL\text{-}G\text{-}F}$ mice in response to DSS treatment compared to their controls (Fig. 6A-D). Similarly, Aβ ELISA of hippocampi demonstrated over a 2-fold increase in both insoluble $A\beta_{1-40}$ and $A\beta_{1-42}$ in DSS treated $App^{NL\text{-}G\text{-}F}$ mice in comparison with the vehicle treated group. Soluble $A\beta_{1-40/42}$ showed no statistically significant changes due to DSS administration, although there was an increase trend in the DSS treated $App^{NL\text{-}G\text{-}F}$ mice (Fig. 6E). These data indicate that inducing moderate intestinal inflammation leads to exacerbation of AD pathology via elevating Aβ plaque deposition and insoluble $A\beta_{1-40/42}$ as a brain change during the recovery phase of DSS treatment in the $App^{NL\text{-}G\text{-}F}$ mice.

Glial immunoreactivity was altered distinctly in $App^{NL\text{-}G\text{-}F}$ and WT mice brains due to the colitis-like symptoms induced by DSS treatment

It is well established that brain specialized inflammatory cells, microglia and astrocytes, become activated and express inflammatory cytokines in various brain diseases, including AD. Impaired microglial phagocytosis activity in response to Aβ plaque deposition plays a hypothesized role in pathogenesis and progression of AD [5, 6, 91–93]. We expected that propagation of gut inflammation induced by DSS to the brain would also affect the brain gliosis correlating with the elevated Aβ levels. Immunohistochemistry was performed to investigate the impact of colonic barrier disruption and gut inflammation on glial activation. Notably, astrocytosis, visualized by using anti-GFAP immunoreactivity, significantly decreased in WT mice but did not reveal any dramatic alterations following DSS administration in $App^{NL\text{-}G\text{-}F}$ mice hippocampi compared to their controls (Fig. 7). Microgliosis was assessed using two different antibodies, anti-Iba-1 and CD68. Interestingly, moderate colonic inflammation diminished Aβ-associated microglial phagocytic phenotype, which is demonstrated by CD68 immunoreactivity, in $App^{NL\text{-}G\text{-}F}$ mice versus their vehicle controls. Similar to GFAP, the microglial protein Iba-1 [94] was not altered in response to gut inflammation induced by DSS in $App^{NL\text{-}G\text{-}F}$ mice hippocampi but significantly increased in WT hippocampi compared to their respective controls (Fig. 7). This suggested that moderate gut inflammation resulted in a selective phenotype change in gliosis, including decreased astrocytosis and increased microgliosis in WT mice and no change in astrocytes but reduced microglial phagocytic phenotype that correlated with increased Aβ plaque accumulation in the $App^{NL\text{-}G\text{-}F}$ brains.

DSS treatment did not change brain cytokine levels

Due to limited remaining hippocampal samples, parietal cortices were lysed and cytokine levels were quantified by ELISA to assess inflammatory cytokine changes in TNF-α, IL-1β, and IL-6 levels as a result of 2 cycles of 2% DSS treatment in both WT and App^{NL-G-F} mice. The brain levels of TNF-α were below the detection level and IL-1β levels were not changed across experimental groups and genotypes (data not shown). As expected, vehicle treated AD mice demonstrated high IL-6 levels. The cytokine levels were not significantly elevated by DSS treatment in either WT or App^{NL-G-F} mice compared to controls, however (Fig. 8). This finding suggests that two rounds of DSS-induced moderate gut inflammation was insufficient to produce elevated changes in select brain cytokines detectable 3 weeks after the last round of treatment.

DSS treated App^{NL-G-F} mice brains demonstrated no changes in neurodegeneration and neuroinflammatory markers

Based upon the changes in Aβ plaque load and microglial CD68 immunoreactivity in App^{NL-G-F} animals as well as gliosis alterations in WT mice due to DSS treatment, we next investigated the changes in levels of proteins involved in Aβ processing and inflammation phenotype in the mouse brains 20 days following the DSS treatments via western blots. Hippocampal lysates were used to quantify APP and BACE (β-secretase) protein levels, two proteins required for Aβ production in AD. No increases were observed in APP and β-secretase protein levels due to gut inflammation in either genotype (Fig. 9). Protein levels of cyclooxygenase-2 (cox-2), an inflammatory marker, were also assessed in the App^{NL-G-F} and WT groups [95]. Similarly, no significant changes were observed in the levels of these proteins following DSS administration (Fig. 9). These results suggest that DSS treatment exerted no sustained effect on additional inflammatory markers in WT and App^{NL-G-F} mice.

DISCUSSION

To the best of our knowledge, this is the first study investigating a direct contribution of colitis-like intestinal inflammation to Aβ plaque levels and glial immunoreactivity using the App^{NL-G-F} transgenic mouse model. We have previously reported that colonic inflammation correlates with brain Aβ plaque deposition starting at 3 months of age in App^{NL-G-F} mice and increased pro-inflammatory markers and macrophages in the ileums of App^{NL-G-F} and APP/PS1 mice compared to controls [34, 35]. In this study, we report that chronic intestinal disruption induced by 2 cycles of DSS exposure resulted in moderate colitis-like symptoms in WT and AD animals with significant motor dysfunction in App^{NL-G-F} mice. Intestinal inflammation correlated with an increase in Aβ plaque load in hippocampi and temporal cortices along with a decrease in microglial CD68 immunoreactivity in App^{NL-G-F} mice during the recovery phase after injury. Taken together, these findings suggest that basal intestinal inflammation, which has been reported in our previous studies, exacerbated by DSS administration in AD animals can propagate to the brain and promote Aβ plaque formation. Based upon the reduced CD68 immunoreactivity, it is intriguing to suggest that increased plaque accumulation may be due to reduced microglial phagocytic phenotype in App^{NL-G-F} mice. Interestingly, induced gut inflammation altered microglial and astrocyte reactivity of WT mice brains uniquely from the App^{NL-G-F} mice. However, due to the age

differences in the wild type and $App^{NL\text{-}G\text{-}F}$ mice we cannot rule out that differences in the response to DSS may well be age dependent and a more rigorous comparison of DSS-mediated effects on the brain in both wild type and $App^{NL\text{-}G\text{-}F}$ mice at similar ages is needed across the lifespan.

Although we do not know how alteration of intestinal function during DSS-induced colitis is specifically causing the brain changes in the $App^{NL\text{-}G\text{-}F}$ mice, human studies support the general notion that colitis influences the brain. For example, it is known that stress can initiate symptomatic flares of IBD based upon a prospective population-based study [96]. In addition, IBD individuals have reduced gray matter volumes and increased white matter hyperintensities in specific brain regions compared to controls [97, 98]. When considering what might be responsible for the intestine to brain communication changes that potentiated some aspects of AD in our study, it is important to remember that the brain and intestine communicate via endocrine, immune, and neuronal mechanisms and the intestinal microbiome appears to play an integral part in regulating these as well [51–65]. Future work will need to systematically assess each pathway to determine relevance in this paradigm.

It is important to point out that we used the DSS-induced colitis model as a general means of driving intestinal inflammation and not to indicate that IBD, per se, influences the risk of AD. DSS, is a negatively charged sulfated polysaccharide that induces intestinal inflammation by disrupting intestinal epithelial integrity to increase colonic permeability leading to translocation of gut microbiota and their metabolites from the lumen into underlying tissue and infiltration of leukocytes into the lamina propria and submucosa followed by the production of pro-inflammatory cytokines [76]. Colonic disruption induced by DSS results in diarrhea, weight loss, and gross rectal bleeding, pathology similar to individuals with ulcerative colitis [99, 100]. This is a controllable, reproducible, simple, and rapid method to induce inflammation and provides the opportunity to study the resolution of inflammation compared to bacterial induction or transgenic models, in which colonic inflammation continues without amelioration. Although we did not explore it in this study, prior work has shown the DSS-induced colitis in mice is critically dependent upon the plasma kallikrein kininogen pathway, or contact system [101]. Importantly, there is clear evidence of disruption of this system in AD. AD patients have demonstrated impaired clotting ability and activation of the contact system [102, 103]. Increased levels of FXII, HK cleavage, and kallikrein activity have all been reported in AD plasma [104]. Aβ and other misfolded proteins can bind to FXII possibly leading to either clot formation via the intrinsic coagulation pathway or increased inflammation via bradykinin generation in AD [104–106]. This Aβ-mediated role of contact system activation in AD is further supported by elevated plasma HK cleavage in a mouse model of AD and wild type mice iv. injected with $A\beta_{42}$ [104] and protection from neuroinflammation in an AD line with Factor XII (FXII) depleted [107]. Further study is required to understand whether activation of the contact system in the DSS paradigm is contributing to the Aβ plaque changes we observed.

Although DSS studies are often performed in younger mice from 6–18 weeks of age [44, 49, 50, 108–117] we elected to use older mice at 24–40 weeks of age to allow us to examine AD-related brain changes. In spite of this older age paradigm, symptomatic parameters, colon histology (erosions and goblet cell loss), changes in CD68 immunohistochemistry

staining, and lipocalin-2 ELISA assessments all demonstrated successful colitis-like pathology induction in both genotypes consistent with other reports [43, 44, 84, 100, 118]. According to Snider and colleagues, mice are expected to recover to their initial weight during the course of recovery [80]. However, neither WT nor $App^{NL\text{-}G\text{-}F}$ animals completely recovered after ending the second cycle of DSS treatment in our paradigm. This could be due to treating mice with DSS at an older age in our study. On the other hand, similar to our data, Chassaing and colleagues reported that weight loss and loose stool continued for 5 weeks after DSS removal in mice on the C57BL/6 background [76]. This suggests that a longer period is required after DSS treatment if a full recovery is desired.

It has been reported that WT animals with DSS-induced colitis show prolonged immobility, abnormal behavioral stress responses, memory impairment, and alterations in expression levels of genes involved in the limbic system [44, 118, 119]. Indeed, we expected to observe exacerbation of memory deficits, at least, in our DSS treated mice. Our OF and CM data revealed a high degree of mobility of the $App^{NL\text{-}G\text{-}F}$ vehicle group. This activity was decreased due to DSS administration observable during the second resolution phase, 12 days post exposure, in the $App^{NL\text{-}G\text{-}F}$ mice. Consistent with our finding of $App^{NL\text{-}G\text{-}F}$ hyperactivity, others have reported increased locomotor activity associated with AD mouse models [120–127] and decreased locomotor activity in $App^{-/-}$ mice [128–130]. Our findings suggest that gut inflammation induced by DSS exposure may affect regions of the brain involved in locomotor activity. However, our OF and CM tests did not demonstrate any anxiety-like or memory deficits due to DSS treatment. It could be that only transient behavioral deficits were induced by DSS-induced inflammation which normalized during the interval phase. Consistent with our data, previous studies reported exacerbation of anxiety-like behavior or memory dysfunction when assessed during active colonic inflammation phase, 0–3 days after DSS cessation. These behavioral changes resolved during the recovery phase even though the colitis-like symptoms, including shortened colon length, colonic histological damages, and increased myeloperoxidase (MPO) activity, were still present [42, 44, 118]. For example, others have shown that WT mice treated with 3% DSS for 5 days demonstrate recognition memory deficits and anxiety-like behavior 3 days post exposure, during active disease, tested by novel object recognition task and light/dark box test, respectively. However, behavior deficits were no longer present 9 days post DSS treatment compared to controls [44]. Similarly, impaired learning and memory in the Y-maze and passive avoidance tasks resolves during recovery of inflammation, 15 days after colitis induced by 2.5% 2,4,6-trinitrobenzenesulfonic acid (TNBS) for 5 days [42]. Taken together, these prior studies indicate that disruption of gut barrier integrity induced by chemicals results in a transient anxiety-like and memory dysfunction which returns to basal levels during the recovery phase. Nevertheless, the prolonged immobility observed in our study may represent gut inflammation-associated major depression which was measured by the tail suspension and forced swimming tests in other studies [131, 132]. More importantly, the long-lasting attenuation in locomotor activity could be attributed to brain responses due to intestinal dysbiosis in $App^{NL\text{-}G\text{-}F}$ versus WT mice basally or resulting from DSS treatment [43, 45–47, 133]. Additional behavioral assessments (movement-limited) and microbiome studies may help to further understand the differences observed. For example,

an improved testing paradigm using a larger open field testing area may have provided a different outcome [89].

Our hypothesis that intestinal dysfunction can manipulate AD related brain changes was only partially supported. We did observe an increase in Aβ plaques although this did not correspond with robust changes in brain cytokines or Iba-1 and GFAP markers of gliosis in $App^{NL\text{-}G\text{-}F}$ mice. Instead, we found a robust decrease in CD68 immunoreactivity in the DSS treated $App^{NL\text{-}G\text{-}F}$ mice. It is unknown why the increase in plaque load and Aβ levels due to DSS treatment did not correlate with increased levels of the proinflammatory cytokines, TNF-α, IL-1β, or IL-6. It is our assumption that changes in brain levels of these cytokines is, in part, due to secretion by glia. Perhaps it is not surprising that DSS treatment did not lead to changes in levels of these cytokines given the lack of increase in markers of gliosis following DSS treatment. This suggests a disconnect between the amyloid deposition and gliosis/cytokine levels in the mice. We expected to observe increased Iba-1, CD68, and GFAP immunoreactivity after DSS treatments as these are commonly used markers for indicating plaque-associated gliosis. It could be that the robust plaque deposition of the $App^{NL\text{-}G\text{-}F}$ line results in a saturation of observable microgliosis and astrocytosis immunoreactivity at the ages used and the minor but significant changes in Aβ plaques is insufficient to elicit a quantifiable change in gliosis and subsequent cytokine changes. Another possibility could be limited sensitivity of our quantitation method, which might only be appropriate to distinguish changes in WT mice that lack the high basal level of microglia and astrocyte immunoreactivities. It could also be that glial immunoreactivity changes in the $App^{NL\text{-}G\text{-}F}$ line were transient and no longer observable during the delayed collection paradigm of 3 weeks post-treatment that we employed. For instance it has been reported that Iba-1 protein levels increased in the hippocampi of 2-month old C57BL/6 females sacrificed 2 days after acute 3% DSS treatment while chronic administration of DSS led to an increase in hippocampal GFAP protein levels with no effect on Iba-1 levels compared to controls [49]. In contrast, another report demonstrated a decrease in GFAP with no significant difference in Iba-1 levels in hippocampi of 6–8 weeks C57BL/6J male mice following 7 days of 2.5% DSS exposure versus controls [134]. Somewhat in agreement with our microglial changes, Iba-1 and CD68 immunoreactivity were reduced in a region-specific manner due to 2% DSS treatment in the hippocampi of adult C57BL/6N males in another report [135]. A more extensive time course profiling of cytokine changes, microglial and astrocyte phenotype markers is clearly required following DSS treatment of $App^{NL\text{-}G\text{-}F}$ mice. Additionally, a more robust colitis paradigm, an unbiased single cell sequencing analysis, or more sensitive quantitation methods to count the numbers and quantify the morphology of plaque-localized microglia or astrocytes might also help clarify whether glial behavior is altered due to colitis-like inflammation.

Conclusion

Taken together, our study suggests that colitis-like inflammation induced by DSS treatment was sufficient to induce long-lasting changes in brain Aβ levels, plaque deposition, and a select marker of microglial phenotype, CD68 immunoreactivity, in the $App^{NL\text{-}G\text{-}F}$ mouse model of AD. Temporal immune, neuronal, and glial characterization of brain changes during repeated intestinal inflammatory bouts early and later in life to model different onsets

of human intestinal disease will provide information regarding whether intestinal inflammation can alter the rate or severity of AD in mice. In addition, identifying the crosstalk mechanisms of communicating intestinal dysfunction to the brain whether it is microbiome, endocrine, immune, or nervous related may identify means of attenuating the peripheral contribution to AD.

Supplementary Material

Refer to Web version on PubMed Central for supplementary material.

ACKNOWLEDGEMENTS

The authors thank Hongyan Wang, the histology technologist in the Department of Pathology, for her assistance with H&E and Alcian blue staining. We appreciate assistance from Jenae Wieser with immunohistochemistry staining and Dr. Kumi Nagamoto-Combs with behavior analysis. The authors would like to thank Dr. Joshua Kulas, Angela Floden, and Dr. Harpreet Kaur for their participation in animal collection. We thank Dr. Michael McDonald, University of Tennessee, for help with analyzing behavioral analysis. The study was supported by NIH/NIA R01AG048993, an Institutional Development Award (IDeA) from the NIH/NIGMS under grant number P20GM103442, and NIH/NIA RF1 AG069378. Histological services were provided by the UND Histology Core Facility supported by the NIH/NIGMS award P20GM113123, DaCCoTA CTR NIH grant U54GM128729, and UND SMHS funds.

REFERENCES

[1]. 2016 Alzheimer's disease facts and figures. Alzheimers Dement 12, 459–509. [PubMed: 27570871]

[2]. Glenner GG, Wong CW (1984) Alzheimer's disease: initial report of the purification and characterization of a novel cerebrovascular amyloid protein. Biochem Biophys Res Commun 120, 885–890. [PubMed: 6375662]

[3]. Terry RD (1963) THE FINE STRUCTURE OF NEUROFIBRILLARY TANGLES IN ALZHEIMER'S DISEASE. J Neuropathol Exp Neurol 22, 629–642. [PubMed: 14069842]

[4]. Beach TG, Walker R, McGeer EG (1989) Patterns of gliosis in Alzheimer's disease and aging cerebrum. Glia 2, 420–436. [PubMed: 2531723]

[5]. Itagaki S, McGeer PL, Akiyama H, Zhu S, Selkoe D (1989) Relationship of microglia and astrocytes to amyloid deposits of Alzheimer disease. J Neuroimmunol 24, 173–182. [PubMed: 2808689]

[6]. Nichols MR, St-Pierre MK, Wendeln AC, Makoni NJ, Gouwens LK, Garrad EC, Sohrabi M, Neher JJ, Tremblay ME, Combs CK (2019) Inflammatory mechanisms in neurodegeneration. J Neurochem 149, 562–581. [PubMed: 30702751]

[7]. Masters CL, Bateman R, Blennow K, Rowe CC, Sperling RA, Cummings JL (2015) Alzheimer's disease. Nat Rev Dis Primers 1, 15056. [PubMed: 27188934]

[8]. Kim HR, Lee P, Seo SW, Roh JH, Oh M, Oh JS, Oh SJ, Kim JS, Jeong Y (2019) Comparison of Amyloid beta and Tau Spread Models in Alzheimer's Disease. Cereb Cortex 29, 4291–4302. [PubMed: 30566579]

[9]. Querfurth HW, LaFerla FM (2010) Alzheimer's disease. N Engl J Med 362, 329–344. [PubMed: 20107219]

[10]. Kohler CA, Maes M, Slyepchenko A, Berk M, Solmi M, Lanctot KL, Carvalho AF (2016) The Gut-Brain Axis, Including the Microbiome, Leaky Gut and Bacterial Translocation: Mechanisms and Pathophysiological Role in Alzheimer's Disease. Curr Pharm Des 22, 6152–6166. [PubMed: 27604604]

[11]. Anand R, Gill KD, Mahdi AA (2014) Therapeutics of Alzheimer's disease: Past, present and future. Neuropharmacology 76 Pt A, 27–50.

[12]. Kinney JW, Bemiller SM, Murtishaw AS, Leisgang AM, Salazar AM, Lamb BT (2018) Inflammation as a central mechanism in Alzheimer's disease. Alzheimers Dement (N Y) 4, 575–590. [PubMed: 30406177]

[13]. Mosher KI, Wyss-Coray T (2014) Microglial dysfunction in brain aging and Alzheimer's disease. Biochem Pharmacol 88, 594–604. [PubMed: 24445162]

[14]. Etminan M, Gill S, Samii A (2003) Effect of non-steroidal anti-inflammatory drugs on risk of Alzheimer's disease: systematic review and meta-analysis of observational studies. Bmj 327, 128. [PubMed: 12869452]

[15]. Wang J, Tan L, Wang HF, Tan CC, Meng XF, Wang C, Tang SW, Yu JT (2015) Anti-inflammatory drugs and risk of Alzheimer's disease: an updated systematic review and meta-analysis. J Alzheimers Dis 44, 385–396. [PubMed: 25227314]

[16]. in t' Veld BA, Ruitenberg A, Hofman A, Launer LJ, van Duijn CM, Stijnen T, Breteler MM, Stricker BH (2001) Nonsteroidal antiinflammatory drugs and the risk of Alzheimer's disease. N Engl J Med 345, 1515–1521. [PubMed: 11794217]

[17]. Zhang C, Wang Y, Wang D, Zhang J, Zhang F (2018) NSAID Exposure and Risk of Alzheimer's Disease: An Updated Meta-Analysis From Cohort Studies. Front Aging Neurosci 10, 83. [PubMed: 29643804]

[18]. Walker KA, Gottesman RF, Wu A, Knopman DS, Gross AL, Mosley TH, Jr., Selvin E, Windham BG (2019) Systemic inflammation during midlife and cognitive change over 20 years: The ARIC Study. Neurology 92, e1256–e1267. [PubMed: 30760633]

[19]. Walker KA, Ficek BN, Westbrook R (2019) Understanding the Role of Systemic Inflammation in Alzheimer's Disease. ACS Chem Neurosci 10, 3340–3342. [PubMed: 31241312]

[20]. Roach M, Christie JA (2008) Fecal incontinence in the elderly. Geriatrics 63, 13–22.

[21]. Leung FW, Rao SS (2009) Fecal incontinence in the elderly. Gastroenterol Clin North Am 38, 503–511. [PubMed: 19699410]

[22]. Schuster BG, Kosar L, Kamrul R (2015) Constipation in older adults: stepwise approach to keep things moving. Can Fam Physician 61, 152–158. [PubMed: 25676646]

[23]. van Hemert S, Skonieczna-Żydecka K, Loniewski I, Szredzki P, Marlicz W (2018) Microscopic colitis-microbiome, barrier function and associated diseases. Ann Transl Med 6, 39. [PubMed: 29610731]

[24]. Holt PR (2001) Diarrhea and malabsorption in the elderly. Gastroenterol Clin North Am 30, 427–444. [PubMed: 11432299]

[25]. Camilleri M, Cowen T, Koch TR (2008) Enteric neurodegeneration in ageing. Neurogastroenterol Motil 20, 418–429. [PubMed: 18371012]

[26]. Navabi S, Gorrepati VS, Yadav S, Chintanaboina J, Maher S, Demuth P, Stern B, Stuart A, Tinsley A, Clarke K, Williams ED, Coates MD (2018) Influences and Impact of Anxiety and Depression in the Setting of Inflammatory Bowel Disease. Inflamm Bowel Dis 24, 2303–2308. [PubMed: 29788469]

[27]. Kurina LM, Goldacre MJ, Yeates D, Gill LE (2001) Depression and anxiety in people with inflammatory bowel disease. J Epidemiol Community Health 55, 716–720. [PubMed: 11553654]

[28]. van Langenberg DR, Yelland GW, Robinson SR, Gibson PR (2017) Cognitive impairment in Crohn's disease is associated with systemic inflammation, symptom burden and sleep disturbance. United European Gastroenterol J 5, 579–587.

[29]. Castaneda AE, Tuulio-Henriksson A, Aronen ET, Marttunen M, Kolho KL (2013) Cognitive functioning and depressive symptoms in adolescents with inflammatory bowel disease. World J Gastroenterol 19, 1611–1617. [PubMed: 23538788]

[30]. Dancey CP, Attree EA, Stuart G, Wilson C, Sonnet A (2009) Words fail me: the verbal IQ deficit in inflammatory bowel disease and irritable bowel syndrome. Inflamm Bowel Dis 15, 852–857. [PubMed: 19130620]

[31]. Attree EA, Dancey CP, Keeling D, Wilson C (2003) Cognitive function in people with chronic illness: inflammatory bowel disease and irritable bowel syndrome. Appl Neuropsychol 10, 96–104. [PubMed: 12788684]

[32]. Zhang B, Wang HE, Bai YM, Tsai SJ, Su TP, Chen TJ, Wang YP, Chen MH (2020) Inflammatory bowel disease is associated with higher dementia risk: a nationwide longitudinal study. Gut.

[33]. Westfall S, Lomis N, Kahouli I, Dia SY, Singh SP, Prakash S (2017) Microbiome, probiotics and neurodegenerative diseases: deciphering the gut brain axis. Cell Mol Life Sci 74, 3769–3787. [PubMed: 28643167]

[34]. Puig KL, Lutz BM, Urquhart SA, Rebel AA, Zhou X, Manocha GD, Sens M, Tuteja AK, Foster NL, Combs CK (2015) Overexpression of mutant amyloid-β protein precursor and presenilin 1 modulates enteric nervous system. J Alzheimers Dis 44, 1263–1278. [PubMed: 25408221]

[35]. Manocha GD, Floden AM, Miller NM, Smith AJ, Nagamoto-Combs K, Saito T, Saido TC, Combs CK (2019) Temporal progression of Alzheimer's disease in brains and intestines of transgenic mice. Neurobiol Aging 81, 166–176. [PubMed: 31284126]

[36]. Khanna S, Tosh PK (2014) A clinician's primer on the role of the microbiome in human health and disease. Mayo Clin Proc 89, 107–114. [PubMed: 24388028]

[37]. Zuo T, Ng SC (2018) The Gut Microbiota in the Pathogenesis and Therapeutics of Inflammatory Bowel Disease. Front Microbiol 9, 2247. [PubMed: 30319571]

[38]. Frank DN, St Amand AL, Feldman RA, Boedeker EC, Harpaz N, Pace NR (2007) Molecular-phylogenetic characterization of microbial community imbalances in human inflammatory bowel diseases. Proc Natl Acad Sci U S A 104, 13780–13785. [PubMed: 17699621]

[39]. Casén C, Vebø HC, Sekelja M, Hegge FT, Karlsson MK, Ciemniejewska E, Dzankovic S, Frøyland C, Nestestog R, Engstrand L, Munkholm P, Nielsen OH, Rogler G, Simrén M, Öhman L, Vatn MH, Rudi K (2015) Deviations in human gut microbiota: a novel diagnostic test for determining dysbiosis in patients with IBS or IBD. Aliment Pharmacol Ther 42, 71–83. [PubMed: 25973666]

[40]. Putignani L, Del Chierico F, Vernocchi P, Cicala M, Cucchiara S, Dallapiccola B (2016) Gut Microbiota Dysbiosis as Risk and Premorbid Factors of IBD and IBS Along the Childhood-Adulthood Transition. Inflamm Bowel Dis 22, 487–504. [PubMed: 26588090]

[41]. Halfvarson J, Brislawn CJ, Lamendella R, Vazquez-Baeza Y, Walters WA, Bramer LM, D'Amato M, Bonfiglio F, McDonald D, Gonzalez A, McClure EE, Dunklebarger MF, Knight R, Jansson JK (2017) Dynamics of the human gut microbiome in inflammatory bowel disease. Nat Microbiol 2, 17004. [PubMed: 28191884]

[42]. Jang SE, Lim SM, Jeong JJ, Jang HM, Lee HJ, Han MJ, Kim DH (2018) Gastrointestinal inflammation by gut microbiota disturbance induces memory impairment in mice. Mucosal Immunol 11, 369–379. [PubMed: 28612842]

[43]. Wang SL, Shao BZ, Zhao SB, Chang X, Wang P, Miao CY, Li ZS, Bai Y (2019) Intestinal autophagy links psychosocial stress with gut microbiota to promote inflammatory bowel disease. Cell Death Dis 10, 391. [PubMed: 31564717]

[44]. Emge JR, Huynh K, Miller EN, Kaur M, Reardon C, Barrett KE, Gareau MG (2016) Modulation of the microbiota-gut-brain axis by probiotics in a murine model of inflammatory bowel disease. Am J Physiol Gastrointest Liver Physiol 310, G989–998. [PubMed: 27056723]

[45]. Vogt NM, Kerby RL, Dill-McFarland KA, Harding SJ, Merluzzi AP, Johnson SC, Carlsson CM, Asthana S, Zetterberg H, Blennow K, Bendlin BB, Rey FE (2017) Gut microbiome alterations in Alzheimer's disease. Sci Rep 7, 13537. [PubMed: 29051531]

[46]. Shen L, Liu L, Ji HF (2017) Alzheimer's Disease Histological and Behavioral Manifestations in Transgenic Mice Correlate with Specific Gut Microbiome State. J Alzheimers Dis 56, 385–390. [PubMed: 27911317]

[47]. Zhang L, Wang Y, Xiayu X, Shi C, Chen W, Song N, Fu X, Zhou R, Xu YF, Huang L, Zhu H, Han Y, Qin C (2017) Altered Gut Microbiota in a Mouse Model of Alzheimer's Disease. J Alzheimers Dis 60, 1241–1257. [PubMed: 29036812]

[48]. Riazi K, Galic MA, Kuzmiski JB, Ho W, Sharkey KA, Pittman QJ (2008) Microglial activation and TNFalpha production mediate altered CNS excitability following peripheral inflammation. Proc Natl Acad Sci U S A 105, 17151–17156. [PubMed: 18955701]

[49]. Zonis S, Pechnick RN, Ljubimov VA, Mahgerefteh M, Wawrowsky K, Michelsen KS, Chesnokova V (2015) Chronic intestinal inflammation alters hippocampal neurogenesis. J Neuroinflammation 12, 65. [PubMed: 25889852]

[50]. Han Y, Zhao T, Cheng X, Zhao M, Gong SH, Zhao YQ, Wu HT, Fan M, Zhu LL (2018) Cortical Inflammation is Increased in a DSS-Induced Colitis Mouse Model. Neurosci Bull 34, 1058–1066. [PubMed: 30225764]

[51]. Cryan JF, O'Mahony SM (2011) The microbiome-gut-brain axis: from bowel to behavior. Neurogastroenterol Motil 23, 187–192. [PubMed: 21303428]

[52]. Harvey L, Boksa P (2012) Prenatal and postnatal animal models of immune activation: relevance to a range of neurodevelopmental disorders. Dev Neurobiol 72, 1335–1348. [PubMed: 22730147]

[53]. Perry VH (2004) The influence of systemic inflammation on inflammation in the brain: implications for chronic neurodegenerative disease. Brain Behav Immun 18, 407–413. [PubMed: 15265532]

[54]. Quan N, Banks WA (2007) Brain-immune communication pathways. Brain Behav Immun 21, 727–735. [PubMed: 17604598]

[55]. Clarke G, O'Mahony SM, Dinan TG, Cryan JF (2014) Priming for health: gut microbiota acquired in early life regulates physiology, brain and behaviour. Acta Paediatr 103, 812–819. [PubMed: 24798884]

[56]. Wallace TC, Guarner F, Madsen K, Cabana MD, Gibson G, Hentges E, Sanders ME (2011) Human gut microbiota and its relationship to health and disease. Nutr Rev 69, 392–403. [PubMed: 21729093]

[57]. Forsythe P, Bienenstock J, Kunze WA (2014) Vagal pathways for microbiome-brain-gut axis communication. Adv Exp Med Biol 817, 115–133. [PubMed: 24997031]

[58]. Fung TC, Olson CA, Hsiao EY (2017) Interactions between the microbiota, immune and nervous systems in health and disease. Nat Neurosci 20, 145–155. [PubMed: 28092661]

[59]. O'Mahony SM, Clarke G, Borre YE, Dinan TG, Cryan JF (2015) Serotonin, tryptophan metabolism and the brain-gut-microbiome axis. Behav Brain Res 277, 32–48. [PubMed: 25078296]

[60]. Strandwitz P (2018) Neurotransmitter modulation by the gut microbiota. Brain Res 1693, 128–133. [PubMed: 29903615]

[61]. Bonaz BL, Bernstein CN (2013) Brain-gut interactions in inflammatory bowel disease. Gastroenterology 144, 36–49. [PubMed: 23063970]

[62]. Dalile B, Van Oudenhove L, Vervliet B, Verbeke K (2019) The role of short-chain fatty acids in microbiota-gut-brain communication. Nat Rev Gastroenterol Hepatol 16, 461–478. [PubMed: 31123355]

[63]. Powell N, Walker MM, Talley NJ (2017) The mucosal immune system: master regulator of bidirectional gut-brain communications. Nat Rev Gastroenterol Hepatol 14, 143–159. [PubMed: 28096541]

[64]. Cryan JF, O'Riordan KJ, Cowan CSM, Sandhu KV, Bastiaanssen TFS, Boehme M, Codagnone MG, Cussotto S, Fulling C, Golubeva AV, Guzzetta KE, Jaggar M, Long-Smith CM, Lyte JM, Martin JA, Molinero-Perez A, Moloney G, Morelli E, Morillas E, O'Connor R, Cruz-Pereira JS, Peterson VL, Rea K, Ritz NL, Sherwin E, Spichak S, Teichman EM, van de Wouw M, Ventura-Silva AP, Wallace-Fitzsimons SE, Hyland N, Clarke G, Dinan TG (2019) The Microbiota-Gut-Brain Axis. Physiol Rev 99, 1877–2013. [PubMed: 31460832]

[65]. Sylvia KE, Demas GE (2018) A gut feeling: Microbiome-brain-immune interactions modulate social and affective behaviors. Horm Behav 99, 41–49. [PubMed: 29427583]

[66]. Maes M, Kubera M, Leunis JC (2008) The gut-brain barrier in major depression: intestinal mucosal dysfunction with an increased translocation of LPS from gram negative enterobacteria (leaky gut) plays a role in the inflammatory pathophysiology of depression. Neuro Endocrinol Lett 29, 117–124. [PubMed: 18283240]

[67]. de Punder K, Pruimboom L (2015) Stress induces endotoxemia and low-grade inflammation by increasing barrier permeability. Front Immunol 6, 223. [PubMed: 26029209]

[68]. Hansen MK, Nguyen KT, Fleshner M, Goehler LE, Gaykema RP, Maier SF, Watkins LR (2000) Effects of vagotomy on serum endotoxin, cytokines, and corticosterone after intraperitoneal lipopolysaccharide. Am J Physiol Regul Integr Comp Physiol 278, R331–336. [PubMed: 10666132]

[69]. Gabele E, Dostert K, Hofmann C, Wiest R, Scholmerich J, Hellerbrand C, Obermeier F (2011) DSS induced colitis increases portal LPS levels and enhances hepatic inflammation and fibrogenesis in experimental NASH. J Hepatol 55, 1391–1399. [PubMed: 21703208]

[70]. Gong Z, Zhao S, Zhou J, Yan J, Wang L, Du X, Li H, Chen Y, Cai W, Wu J (2018) Curcumin alleviates DSS-induced colitis via inhibiting NLRP3 inflammsome activation and IL-1beta production. Mol Immunol 104, 11–19. [PubMed: 30396035]

[71]. Ng A, Tam WW, Zhang MW, Ho CS, Husain SF, McIntyre RS, Ho RC (2018) IL-1beta, IL-6, TNF- alpha and CRP in Elderly Patients with Depression or Alzheimer's disease: Systematic Review and Meta-Analysis. Sci Rep 8, 12050. [PubMed: 30104698]

[72]. Dowlati Y, Herrmann N, Swardfager W, Liu H, Sham L, Reim EK, Lanctot KL (2010) A meta-analysis of cytokines in major depression. Biol Psychiatry 67, 446–457. [PubMed: 20015486]

[73]. Saito T, Matsuba Y, Mihira N, Takano J, Nilsson P, Itohara S, Iwata N, Saido TC (2014) Single App knock-in mouse models of Alzheimer's disease. Nat Neurosci 17, 661–663. [PubMed: 24728269]

[74]. Kim JJ, Shajib MS, Manocha MM, Khan WI (2012) Investigating intestinal inflammation in DSS-induced model of IBD. J Vis Exp.

[75]. Wirtz S, Popp V, Kindermann M, Gerlach K, Weigmann B, Fichtner-Feigl S, Neurath MF (2017) Chemically induced mouse models of acute and chronic intestinal inflammation. Nat Protoc 12, 1295–1309. [PubMed: 28569761]

[76]. Chassaing B, Aitken JD, Malleshappa M, Vijay-Kumar M (2014) Dextran sulfate sodium (DSS)-induced colitis in mice. Curr Protoc Immunol 104, Unit 15.25.

[77]. Cooper HS, Murthy SN, Shah RS, Sedergran DJ (1993) Clinicopathologic study of dextran sulfate sodium experimental murine colitis. Lab Invest 69, 238–249. [PubMed: 8350599]

[78]. Eichele DD, Kharbanda KK (2017) Dextran sodium sulfate colitis murine model: An indispensable tool for advancing our understanding of inflammatory bowel diseases pathogenesis. World J Gastroenterol 23, 6016–6029. [PubMed: 28970718]

[79]. Ghia JE, Blennerhassett P, Kumar-Ondiveeran H, Verdu EF, Collins SM (2006) The vagus nerve: a tonic inhibitory influence associated with inflammatory bowel disease in a murine model. Gastroenterology 131, 1122–1130. [PubMed: 17030182]

[80]. Snider AJ, Bialkowska AB, Ghaleb AM, Yang VW, Obeid LM, Hannun YA (2016) Murine Model for Colitis-Associated Cancer of the Colon. Methods Mol Biol 1438, 245–254. [PubMed: 27150094]

[81]. Sohrabi M, Combs CK (2019) A protocol for making and sectioning multiple embedded Swiss-rolls in a gelatin matrix. MethodsX 6, 2028–2036. [PubMed: 31667100]

[82]. Erben U, Loddenkemper C, Doerfel K, Spieckermann S, Haller D, Heimesaat MM, Zeitz M, Siegmund B, Kühl AA (2014) A guide to histomorphological evaluation of intestinal inflammation in mouse models. Int J Clin Exp Pathol 7, 4557–4576. [PubMed: 25197329]

[83]. Nagamoto-Combs K, Manocha GD, Puig K, Combs CK (2016) An improved approach to align and embed multiple brain samples in a gelatin-based matrix for simultaneous histological processing. J Neurosci Methods 261, 155–160. [PubMed: 26743972]

[84]. Chassaing B, Srinivasan G, Delgado MA, Young AN, Gewirtz AT, Vijay-Kumar M (2012) Fecal lipocalin 2, a sensitive and broadly dynamic non-invasive biomarker for intestinal inflammation. PLoS One 7, e44328. [PubMed: 22957064]

[85]. Adams GG, Dilly PN (1989) Differential staining of ocular goblet cells. Eye (Lond) 3 (Pt 6), 840–844.

[86]. Rugtveit J, Brandtzaeg P, Halstensen TS, Fausa O, Scott H (1994) Increased macrophage subset in inflammatory bowel disease: apparent recruitment from peripheral blood monocytes. Gut 35, 669–674. [PubMed: 8200563]

[87]. Kjeldsen L, Cowland JB, Borregaard N (2000) Human neutrophil gelatinase-associated lipocalin and homologous proteins in rat and mouse. Biochim Biophys Acta 1482, 272–283. [PubMed: 11058768]

[88]. Crawley JN (1985) Exploratory behavior models of anxiety in mice. Neurosci Biobehav Rev 9, 37–44. [PubMed: 2858080]

[89]. Shieh KR, Yang SC (2019) Exploratory and agile behaviors with central dopaminergic activities in open field tests in Formosan wood mice (Apodemus semotus). J Exp Biol 222.

[90]. Wang B, Liu Y, Huang L, Chen J, Li JJ, Wang R, Kim E, Chen Y, Justicia C, Sakata K, Chen H, Planas A, Ostrom RS, Li W, Yang G, McDonald MP, Chen R, Heck DH, Liao FF (2017) A CNS-permeable Hsp90 inhibitor rescues synaptic dysfunction and memory loss in APP-overexpressing Alzheimer's mouse model via an HSF1-mediated mechanism. Mol Psychiatry 22, 990–1001. [PubMed: 27457810]

[91]. Hansen DV, Hanson JE, Sheng M (2018) Microglia in Alzheimer's disease. J Cell Biol 217, 459–472. [PubMed: 29196460]

[92]. Prinz M, Priller J, Sisodia SS, Ransohoff RM (2011) Heterogeneity of CNS myeloid cells and their roles in neurodegeneration. Nat Neurosci 14, 1227–1235. [PubMed: 21952260]

[93]. Wang WY, Tan MS, Yu JT, Tan L (2015) Role of pro-inflammatory cytokines released from microglia in Alzheimer's disease. Ann Transl Med 3, 136. [PubMed: 26207229]

[94]. Franco-Bocanegra DK, McAuley C, Nicoll JAR, Boche D (2019) Molecular Mechanisms of Microglial Motility: Changes in Ageing and Alzheimer's Disease. Cells 8.

[95]. Chung DW, Yoo KY, Hwang IK, Kim DW, Chung JY, Lee CH, Choi JH, Choi SY, Youn HY, Lee IS, Won MH (2010) Systemic administration of lipopolysaccharide induces cyclooxygenase-2 immunoreactivity in endothelium and increases microglia in the mouse hippocampus. Cell Mol Neurobiol 30, 531–541. [PubMed: 19908141]

[96]. Bernstein CN, Singh S, Graff LA, Walker JR, Miller N, Cheang M (2010) A prospective population-based study of triggers of symptomatic flares in IBD. Am J Gastroenterol 105, 1994–2002. [PubMed: 20372115]

[97]. Agostini A, Benuzzi F, Filippini N, Bertani A, Scarcelli A, Farinelli V, Marchetta C, Calabrese C, Rizzello F, Gionchetti P, Ercolani M, Campieri M, Nichelli P (2013) New insights into the brain involvement in patients with Crohn's disease: a voxel-based morphometry study. Neurogastroenterol Motil 25, 147–e182. [PubMed: 22998431]

[98]. Zikou AK, Kosmidou M, Astrakas LG, Tzarouchi LC, Tsianos E, Argyropoulou MI (2014) Brain involvement in patients with inflammatory bowel disease: a voxel-based morphometry and diffusion tensor imaging study. Eur Radiol 24, 2499–2506. [PubMed: 25001084]

[99]. Okayasu I, Hatakeyama S, Yamada M, Ohkusa T, Inagaki Y, Nakaya R (1990) A novel method in the induction of reliable experimental acute and chronic ulcerative colitis in mice. Gastroenterology 98, 694–702. [PubMed: 1688816]

[100]. Perše M, Cerar A (2012) Dextran sodium sulphate colitis mouse model: traps and tricks. J Biomed Biotechnol 2012, 718617. [PubMed: 22665990]

[101]. Wang B, Yang A, Zhao Z, He C, Liu Y, Colman RW, Dai J, Wu Y (2018) The Plasma Kallikrein-Kininogen Pathway Is Critical in the Pathogenesis of Colitis in Mice. Front Immunol 9, 21. [PubMed: 29467753]

[102]. Suidan GL, Singh PK, Patel-Hett S, Chen ZL, Volfson D, Yamamoto-Imoto H, Norris EH, Bell RD, Strickland S (2018) Abnormal clotting of the intrinsic/contact pathway in Alzheimer disease patients is related to cognitive ability. Blood Adv 2, 954–963. [PubMed: 29700007]

[103]. Bergamaschini L, Parnetti L, Pareyson D, Canziani S, Cugno M, Agostoni A (1998) Activation of the contact system in cerebrospinal fluid of patients with Alzheimer disease. Alzheimer Dis Assoc Disord 12, 102–108. [PubMed: 9651139]

[104]. Zamolodchikov D, Chen ZL, Conti BA, Renne T, Strickland S (2015) Activation of the factor XII-driven contact system in Alzheimer's disease patient and mouse model plasma. Proc Natl Acad Sci U S A 112, 4068–4073. [PubMed: 25775543]

[105]. Maas C, Govers-Riemslag JW, Bouma B, Schiks B, Hazenberg BP, Lokhorst HM, Hammarstrom P, ten Cate H, de Groot PG, Bouma BN, Gebbink MF (2008) Misfolded proteins activate factor XII in humans, leading to kallikrein formation without initiating coagulation. J Clin Invest 118, 3208–3218. [PubMed: 18725990]

[106]. Zamolodchikov D, Renne T, Strickland S (2016) The Alzheimer's disease peptide beta-amyloid promotes thrombin generation through activation of coagulation factor XII. J Thromb Haemost 14, 995–1007. [PubMed: 26613657]

[107]. Chen ZL, Revenko AS, Singh P, MacLeod AR, Norris EH, Strickland S (2017) Depletion of coagulation factor XII ameliorates brain pathology and cognitive impairment in Alzheimer disease mice. Blood 129, 2547–2556. [PubMed: 28242605]

[108]. Bercik P, Park AJ, Sinclair D, Khoshdel A, Lu J, Huang X, Deng Y, Blennerhassett PA, Fahnestock M, Moine D, Berger B, Huizinga JD, Kunze W, McLean PG, Bergonzelli GE, Collins SM, Verdu EF (2011) The anxiolytic effect of Bifidobacterium longum NCC3001 involves vagal pathways for gut-brain communication. Neurogastroenterol Motil 23, 1132–1139. [PubMed: 21988661]

[109]. Loren V, Manye J, Fuentes MC, Cabre E, Ojanguren I, Espadaler J (2017) Comparative Effect of the I3.1 Probiotic Formula in Two Animal Models of Colitis. Probiotics Antimicrob Proteins 9, 71–80. [PubMed: 27832441]

[110]. Hassan AM, Jain P, Reichmann F, Mayerhofer R, Farzi A, Schuligoi R, Holzer P (2014) Repeated predictable stress causes resilience against colitis-induced behavioral changes in mice. Front Behav Neurosci 8, 386. [PubMed: 25414650]

[111]. Jirkof P, Leucht K, Cesarovic N, Caj M, Nicholls F, Rogler G, Arras M, Hausmann M (2013) Burrowing is a sensitive behavioural assay for monitoring general wellbeing during dextran sulfate sodium colitis in laboratory mice. Lab Anim 47, 274–283. [PubMed: 23828853]

[112]. Mar JS, Nagalingam NA, Song Y, Onizawa M, Lee JW, Lynch SV (2014) Amelioration of DSS-induced murine colitis by VSL#3 supplementation is primarily associated with changes in ileal microbiota composition. Gut Microbes 5, 494–503. [PubMed: 25144681]

[113]. Kumar M, Kissoon-Singh V, Coria AL, Moreau F, Chadee K (2017) Probiotic mixture VSL#3 reduces colonic inflammation and improves intestinal barrier function in Muc2 mucin-deficient mice. Am J Physiol Gastrointest Liver Physiol 312, G34–g45. [PubMed: 27856417]

[114]. Mitrovic M, Shahbazian A, Bock E, Pabst MA, Holzer P (2010) Chemo-nociceptive signalling from the colon is enhanced by mild colitis and blocked by inhibition of transient receptor potential ankyrin 1 channels. Br J Pharmacol 160, 1430–1442. [PubMed: 20590633]

[115]. Villaran RF, Espinosa-Oliva AM, Sarmiento M, De Pablos RM, Arguelles S, Delgado-Cortes MJ, Sobrino V, Van Rooijen N, Venero JL, Herrera AJ, Cano J, Machado A (2010) Ulcerative colitis exacerbates lipopolysaccharide-induced damage to the nigral dopaminergic system: potential risk factor in Parkinson`s disease. J Neurochem 114, 1687–1700. [PubMed: 20584104]

[116]. Lu F, Fernandes SM, Davis AE, 3rd (2010) The role of the complement and contact systems in the dextran sulfate sodium-induced colitis model: the effect of C1 inhibitor in inflammatory bowel disease. Am J Physiol Gastrointest Liver Physiol 298, G878–883. [PubMed: 20338925]

[117]. Di Martino L, Dave M, Menghini P, Xin W, Arseneau KO, Pizarro TT, Cominelli F (2016) Protective Role for TWEAK/Fn14 in Regulating Acute Intestinal Inflammation and Colitis-Associated Tumorigenesis. Cancer Res 76, 6533–6542. [PubMed: 27634763]

[118]. Reichmann F, Hassan AM, Farzi A, Jain P, Schuligoi R, Holzer P (2015) Dextran sulfate sodium-induced colitis alters stress-associated behaviour and neuropeptide gene expression in the amygdala-hippocampus network of mice. Sci Rep 5, 9970. [PubMed: 26066467]

[119]. Reichmann F, Painsipp E, Holzer P (2013) Environmental enrichment and gut inflammation modify stress-induced c-Fos expression in the mouse corticolimbic system. PLoS One 8, e54811. [PubMed: 23349972]

[120]. Dodart JC, Meziane H, Mathis C, Bales KR, Paul SM, Ungerer A (1999) Behavioral disturbances in transgenic mice overexpressing the V717F beta-amyloid precursor protein. Behav Neurosci 113, 982–990. [PubMed: 10571480]

[121]. King DL, Arendash GW, Crawford F, Sterk T, Menendez J, Mullan MJ (1999) Progressive and gender-dependent cognitive impairment in the APP(SW) transgenic mouse model for Alzheimer's disease. Behav Brain Res 103, 145–162. [PubMed: 10513583]

[122]. Arendash GW, King DL, Gordon MN, Morgan D, Hatcher JM, Hope CE, Diamond DM (2001) Progressive, age-related behavioral impairments in transgenic mice carrying both mutant amyloid precursor protein and presenilin-1 transgenes. Brain Res 891, 42–53. [PubMed: 11164808]

[123]. Dumont M, Strazielle C, Staufenbiel M, Lalonde R (2004) Spatial learning and exploration of environmental stimuli in 24-month-old female APP23 transgenic mice with the Swedish mutation. Brain Res 1024, 113–121. [PubMed: 15451372]

[124]. Hyde LA, Kazdoba TM, Grilli M, Lozza G, Brusa R, Zhang Q, Wong GT, McCool MF, Zhang L, Parker EM, Higgins GA (2005) Age-progressing cognitive impairments and neuropathology in transgenic CRND8 mice. Behav Brain Res 160, 344–355. [PubMed: 15863231]

[125]. Lalonde R, Lewis TL, Strazielle C, Kim H, Fukuchi K (2003) Transgenic mice expressing the betaAPP695SWE mutation: effects on exploratory activity, anxiety, and motor coordination. Brain Res 977, 38–45. [PubMed: 12788511]

[126]. Gil-Bea FJ, Aisa B, Schliebs R, Ramírez MJ (2007) Increase of locomotor activity underlying the behavioral disinhibition in tg2576 mice. Behav Neurosci 121, 340–344. [PubMed: 17469923]

[127]. Pietropaolo S, Feldon J, Yee BK (2008) Age-dependent phenotypic characteristics of a triple transgenic mouse model of Alzheimer disease. Behav Neurosci 122, 733–747. [PubMed: 18729626]

[128]. Zheng H, Jiang M, Trumbauer ME, Sirinathsinghji DJ, Hopkins R, Smith DW, Heavens RP, Dawson GR, Boyce S, Conner MW, Stevens KA, Slunt HH, Sisoda SS, Chen HY, Van der Ploeg LH (1995) beta-Amyloid precursor protein-deficient mice show reactive gliosis and decreased locomotor activity. Cell 81, 525–531. [PubMed: 7758106]

[129]. Dawson GR, Seabrook GR, Zheng H, Smith DW, Graham S, O'Dowd G, Bowery BJ, Boyce S, Trumbauer ME, Chen HY, Van der Ploeg LH, Sirinathsinghji DJ (1999) Age-related cognitive deficits, impaired long-term potentiation and reduction in synaptic marker density in mice lacking the beta-amyloid precursor protein. Neuroscience 90, 1–13. [PubMed: 10188929]

[130]. Ring S, Weyer SW, Kilian SB, Waldron E, Pietrzik CU, Filippov MA, Herms J, Buchholz C, Eckman CB, Korte M, Wolfer DP, Müller UC (2007) The secreted beta-amyloid precursor protein ectodomain APPs alpha is sufficient to rescue the anatomical, behavioral, and electrophysiological abnormalities of APP-deficient mice. J Neurosci 27, 7817–7826. [PubMed: 17634375]

[131]. Cryan JF, Mombereau C, Vassout A (2005) The tail suspension test as a model for assessing antidepressant activity: review of pharmacological and genetic studies in mice. Neurosci Biobehav Rev 29, 571–625. [PubMed: 15890404]

[132]. Petit-Demouliere B, Chenu F, Bourin M (2005) Forced swimming test in mice: a review of antidepressant activity. Psychopharmacology (Berl) 177, 245–255. [PubMed: 15609067]

[133]. Håkansson Å, Tormo-Badia N, Baridi A, Xu J, Molin G, Hagslätt ML, Karlsson C, Jeppsson B, Cilio CM, Ahrné S (2015) Immunological alteration and changes of gut microbiota after dextran sulfate sodium (DSS) administration in mice. Clin Exp Med 15, 107–120. [PubMed: 24414342]

[134]. Zhang N, Zhang Q, Xie L, Li C, Zhuang Z, Lin S, Lv P, Liu Y, Wu Q, Yu S (2020) Electroacupuncture and Moxibustion Regulate Hippocampus Glia and Mitochondria Activation in DSS-Induced Colitis Mice. Evid Based Complement Alternat Med 2020, 2530253. [PubMed: 32047521]

[135]. Sroor HM, Hassan AM, Zenz G, Valadez-Cosmes P, Farzi A, Holzer P, El-Sharif A, Gomaa FAM, Kargl J, Reichmann F (2019) Experimental colitis reduces microglial cell activation in the mouse brain without affecting microglial cell numbers. Sci Rep 9, 20217. [PubMed: 31882991]

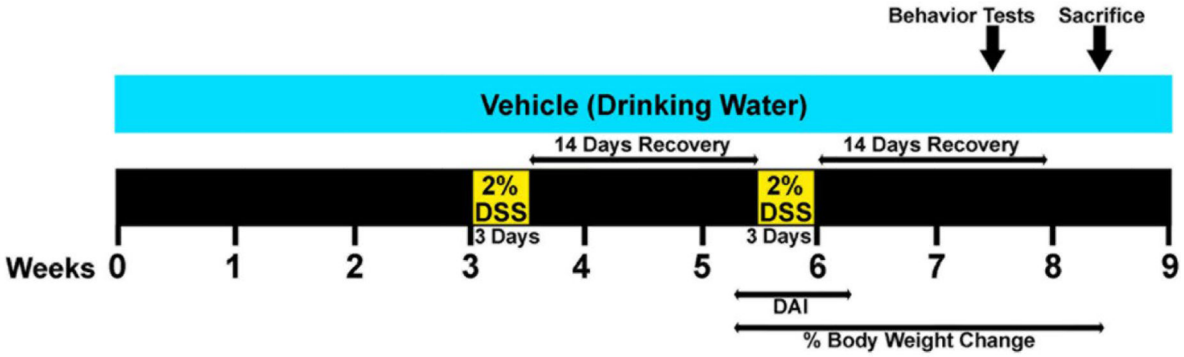

Fig. 1.

Schematic of the experimental design and timeline of DSS treatments and different assessments. 2% DSS was dissolved in the drinking water and fed *ad libitum* to male C57BL/6 WT and $App^{NL\text{-}G\text{-}F}$ mice (AD mouse model) at 6–10 months of age for 2 cycles of three days each. DAI was scored from 1 day pre exposure to 2 days post exposure during the second bout of DSS treatment. The percentage of body weight loss was calculated starting from the second DSS treatment untill the week of euthanasia. On week 7, 12 days after exposure of DSS, mice were tested for behavioral functions. On the following week, brain, colon, and spleen tissues were collected in order to examine the effect of gut integrity disruption during the inflammation resolving phase

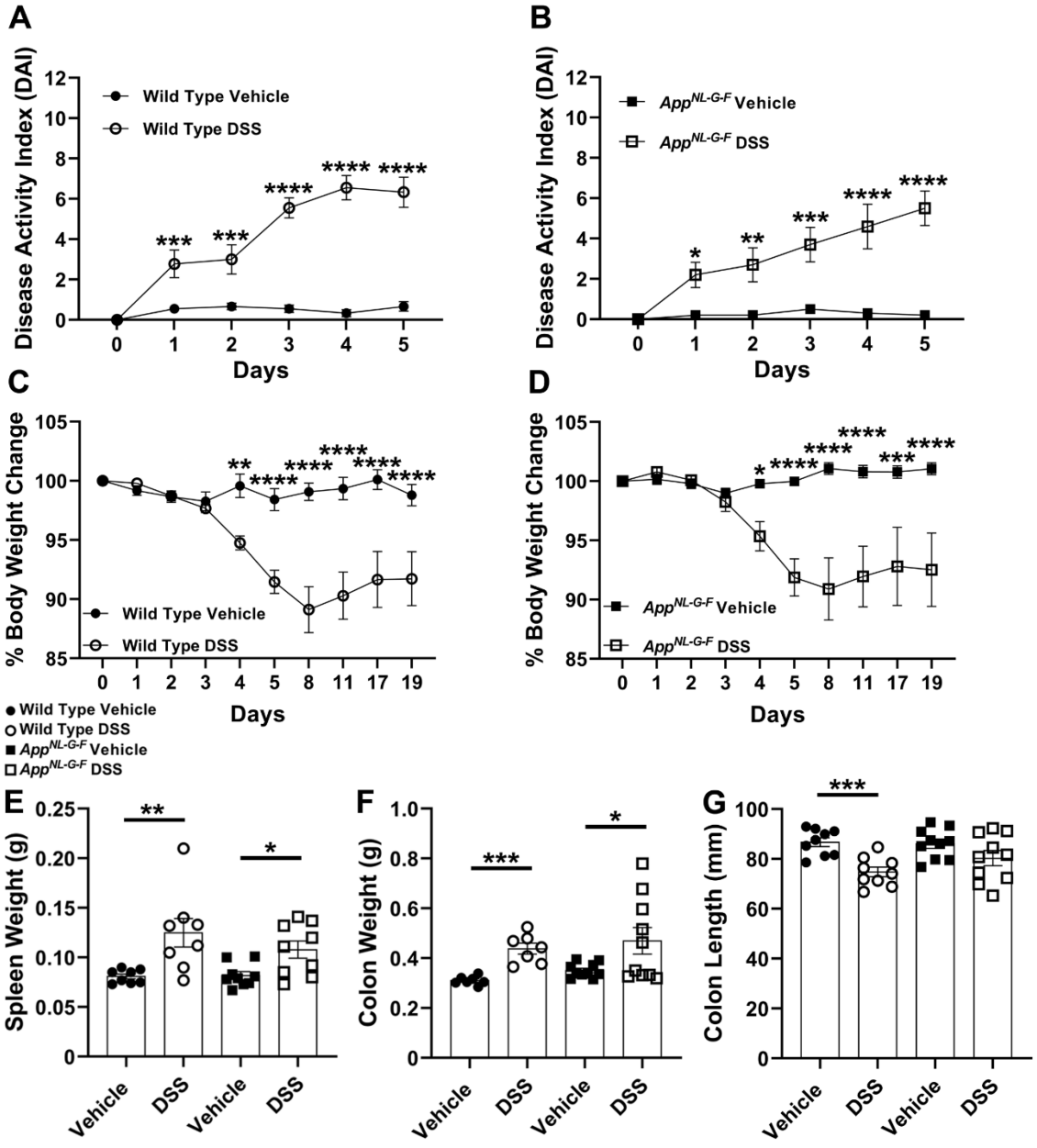

Fig. 2.

DSS treatment induced symptomatic parameters of colitis-like disease in both genotypes compared to controls. (A, B) DAI was monitored on day 0, during the second cycle of 2%DSS (3 days), and 2 days post DSS exposure in both DSS and vehicle treated groups per genotype, (*p<0.05, **p<0.01, ***p<0.001, ****p<0.0001 vehicle treated groups vs. DSS treated groups per genotype comparing on the same day, two-way ANOVA multiple comparisons followed by uncorrected Fisher's LSD test indicate WT DAI F (5, 96) = 15.17 and p (interaction) <0.0001; *App*$^{NL\text{-}G\text{-}F}$ DAI F (5, 108) = 5.272 and p (interaction)= 0.0002, mean ± SEM, n=9–10 animals). (C, D) the percentage of body weight (%BW) changes was calculated during the second DSS exposure untill the week of tissue collection per each treatment groups per genotype, (*p<0.05, **p<0.01, ***p<0.001, ****p<0.0001 vehicle

treated groups vs. DSS treated groups per genotype comparing on the same day, Two-way ANOVA multiple comparisons followed by uncorrected Fisher's LSD test indicate WT %BW F (9, 160) = 6.897 and p (interaction) <0.0001; *App*$^{NL\text{-}G\text{-}F}$ %BW F (9, 180) = 4.798 and p (interaction) <0.0001, mean ± SEM, n=9–10 animals). (E-G) Spleen and colon weights as well as colon length were measured from WT and *App*$^{NL\text{-}G\text{-}F}$ mice to indicate colonic inflammation, (*p<0.05, **p<0.01, ***p<0.001, Unpaired two-tailed t-test indicate WT spleen weight t(14)=3.007 and p=0.0094; *App*$^{NL\text{-}G\text{-}F}$ spleen weight t(16)=2.741 and p=0.0145; WT colon weight t(12)=5.591 and p=0.0001; *App*$^{NL\text{-}G\text{-}F}$ colon weight t(18)=2.215 and p=0.0399; WT colon length t(16)=4.589 and p=0.0003; *App*$^{NL\text{-}G\text{-}F}$ colon length t(18)=1.614 and p=0.1239, mean ± SEM, n=7–10 animals).

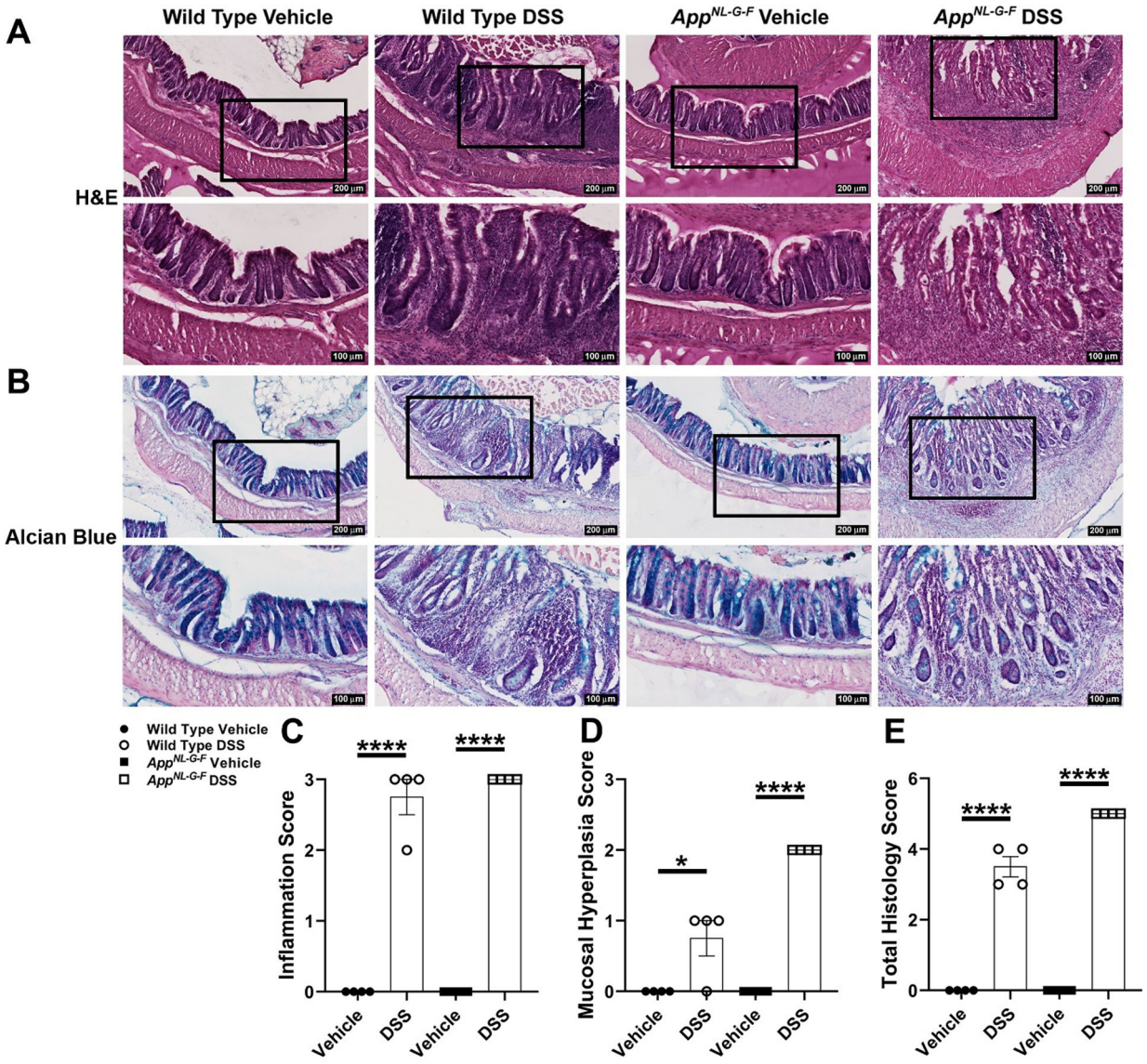

Fig. 3.

DSS treatment resulted in colonic inflammation in both WT and *App*$^{NL\text{-}G\text{-}F}$ mice. (A, B) Representative H&E and Alcian blue staining of cross-sectional Swiss-rolls from the distal colon are shown with 10X and 20X magnifications. Histological examination of H&E staining was performed by scoring (C) inflammation, (D) mucosal hyperplasia, and (E) total histology lesions to indicate the extent and severity of inflammation as well as reduction of goblet cells in colon sections of DSS treated vs. vehicle groups in both genotypes, (*$p<0.05$, ****$p<0.0001$, unpaired two-tailed t-test indicate WT inflammation score $t(6)=11$ and $p<0.0001$; *App*$^{NL\text{-}G\text{-}F}$ inflammation score $t(6)=1.200e+025$ and $p<0.0001$; WT mucosal hyperplasia score $t(6)=3$ and $p=0.0240$; *App*$^{NL\text{-}G\text{-}F}$ mucosal hyperplasia score $t(6)=8.000e+024$ and $p<0.0001$; WT total histology score $t(6)=12.12$ and $p<0.0001$; *App*$^{NL\text{-}G\text{-}F}$ total histology score $t(6)=2.000e+025$ and $p<0.0001$, mean ± SEM, n=4 Swiss-rolls/condition/genotype animals).

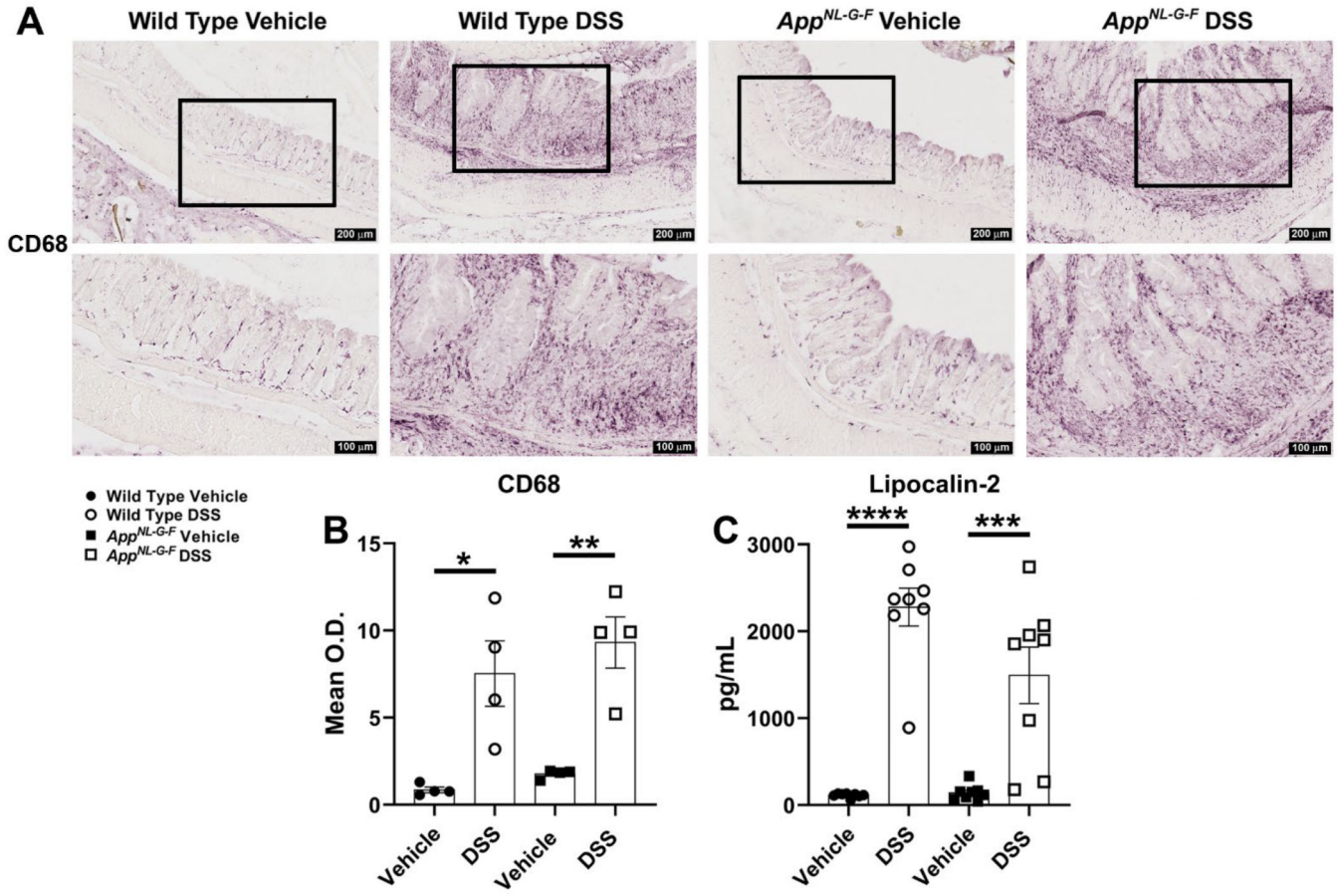

Fig. 4.

DSS treatment led to infiltration of macrophages and increased levels of an inflammatory marker in the colon. (A) Representative anti-CD68 immunostaining of cross sectional Swiss-rolls of the distal colon are shown with 10X and 20X magnifications. (B) CD68 mean optical density was measured using colon sections of DSS treated vs. vehicle groups in both genotypes, (*$p<0.05$, **$p<0.01$, unpaired two-tailed t-test indicate WT CD68 $t(6)=3.547$ and $p=0.0121$; *App*$^{NL\text{-}G\text{-}F}$ CD68 $t(6)=5.112$ and $p=0.0022$, mean ± SEM, n= 4 Swiss-rolls/condition/genotype). (C) The changes in lipocalin-2 levels, as an anti-microbial siderophore-binding peptide involved in IBD, were assessed to determine the extent of intestinal inflammation in both the WT and AD mouse model following DSS exposure, (***$p<0.001$, ****$p<0.0001$, unpaired two-tailed t-test indicate WT lipocalin-2 $t(14)=9.931$ and $p<0.0001$; *App*$^{NL\text{-}G\text{-}F}$ lipocalin-2 $t(14)=4.151$ and $p=0.0010$, mean ± SEM, n=8 animals).

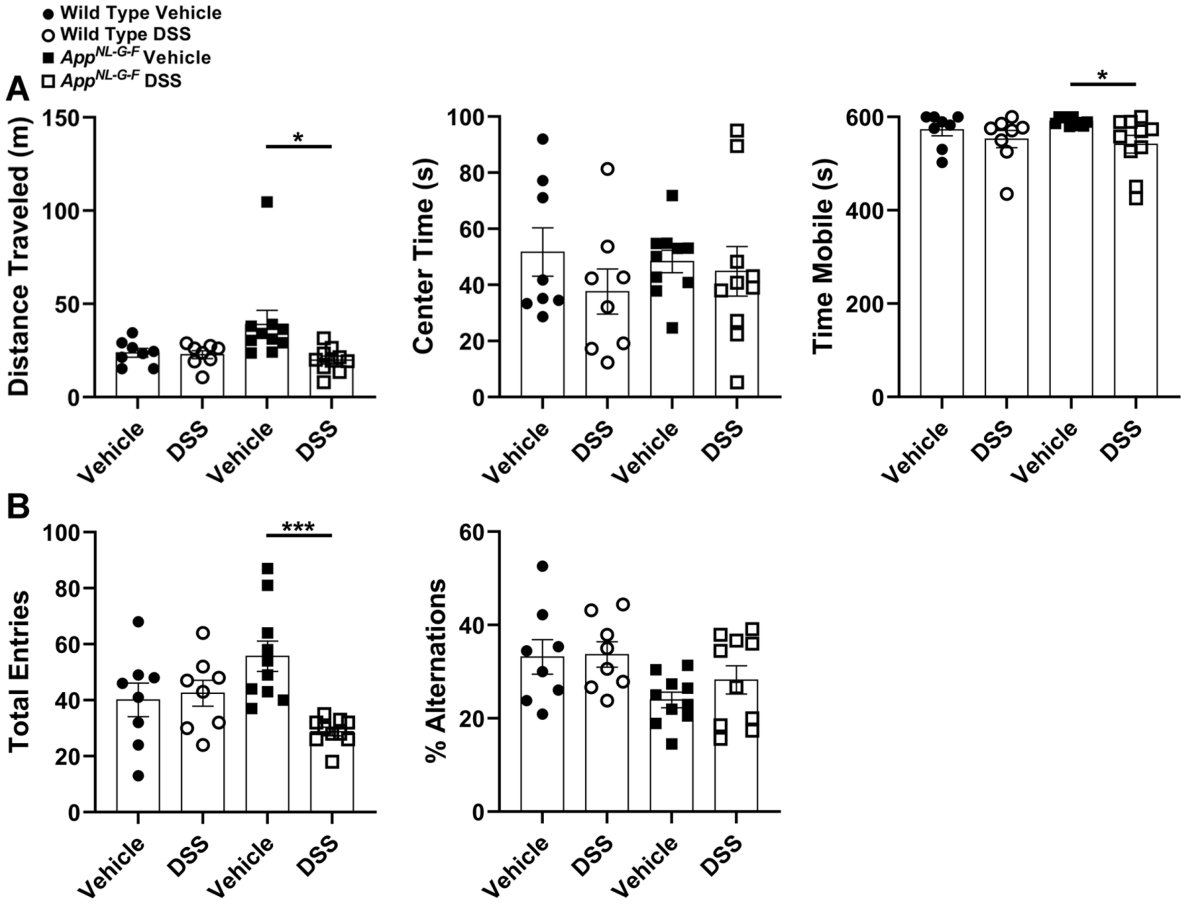

Fig. 5.

DSS treatment decreased mobility of *App*$^{NL-G-F}$ mice in both OF and CM tests. (A) General locomotor activity or anxiety-like behavior was assessed by quantifying the distance traveled, time spent in the center as well as time mobile using the OF test, (*p<0.05, unpaired two-tailed t-test indicate WT distance traveled t(14)=0.3041 and p=0.7655; *App*$^{NL-G-F}$ distance traveled t(18)=2.469 and p=0.0238; WT center time t(14)=1.192 and p=0.2531; *App*$^{NL-G-F}$ center time t(18)=0.3665 and p=0.7182; WT time mobile t(14)=0.8874 and p=0.3898; *App*$^{NL-G-F}$ time mobile t(18)=2.553 and p=0.0200, mean ± SEM, n=8–10 animals tested at 8–12 months of age). (B) Total entries (locomotion) and percentage of alternations in different arms of the CM test were quantified to evaluate working memory in both genotype vehicle and DSS treated groups, (***p<0.001, unpaired two-tailed t-test indicate WT total entries t(14)=0.3129 and p=0.7590; *App*$^{NL-G-F}$ total entries t(18)=4.782 and p=0.0001; WT %alternations t(14)=0.1080 and p=0.9155; *App*$^{NL-G-F}$ %alternations t(18)=1.243 and p=0.2299, mean ± SEM, n=8–10 animals tested at 8–12 months of age).

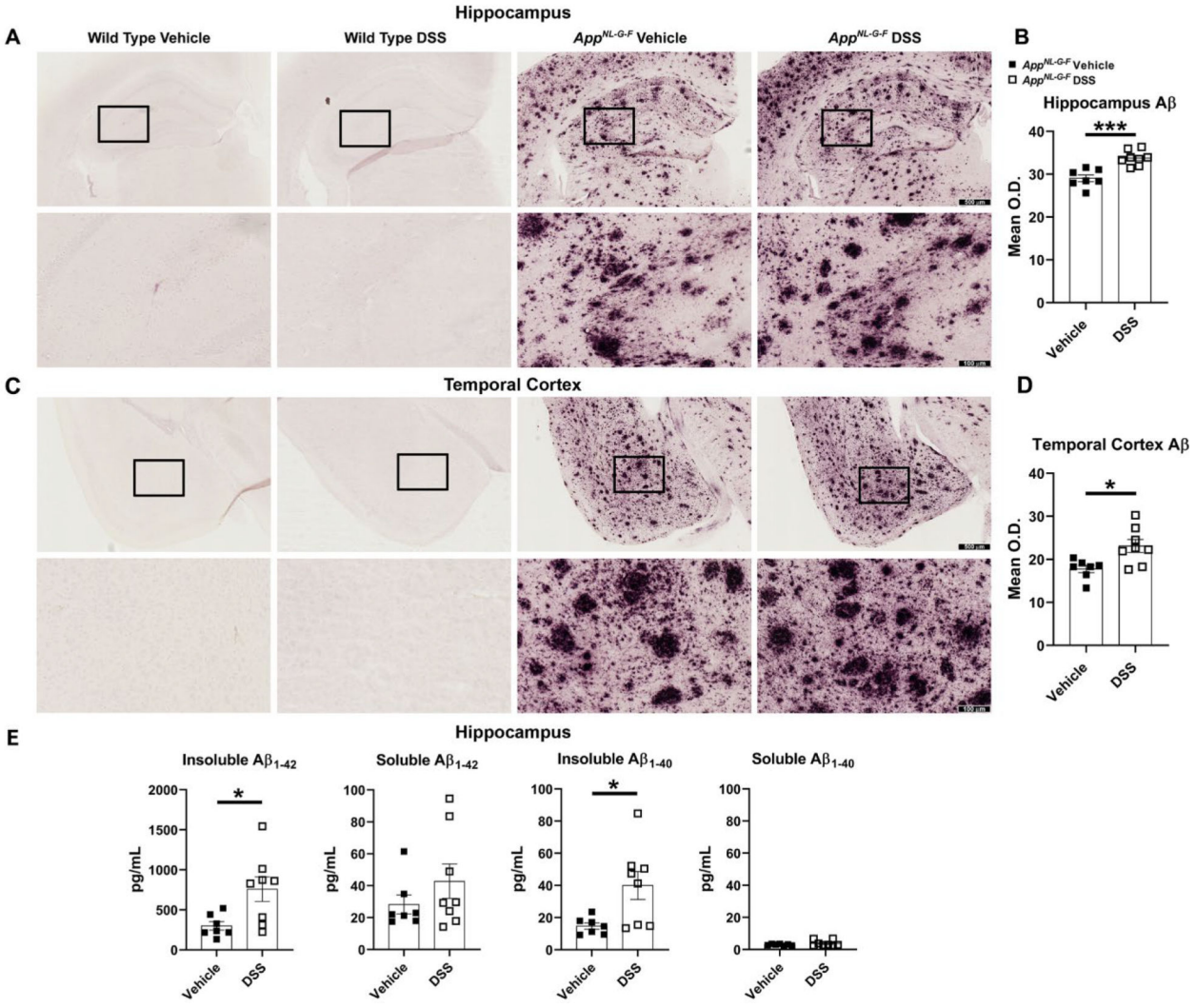

Fig. 6.

DSS treatment elevated hippocampal and temporal cortex Aβ levels in *App*$^{NL\text{-}G\text{-}F}$ mice. (A, C) Immunohistochemistry was performed on both WT and *App*$^{NL\text{-}G\text{-}F}$ brains using anti-Aβ antibody. Representative hippocampi and temporal cortices are shown with 4X and 20X magnifications. (B, D) Mean optical density value was measured using 3 sections of hippocampus or temporal cortex/mouse/condition, (*p<0.05, ***p<0.001, unpaired two-tailed t-test indicate *App*$^{NL\text{-}G\text{-}F}$ hippocampus Aβ t(13)=4.821 and p=0.0003; *App*$^{NL\text{-}G\text{-}F}$ temporal cortex Aβ t(13)=2.969 and p=0.0109, mean ± SEM, n=7–8 animals). (E) Hippocampi, collected from vehicle and DSS treated WT and *App*$^{NL\text{-}G\text{-}F}$ mice, were lysed to perform ELISAs for human insoluble $A\beta_{1–40/42}$ and soluble $A\beta_{1–40/42}$, (*p<0.05, unpaired two-tailed t-test indicate *App*$^{NL\text{-}G\text{-}F}$ insoluble $A\beta_{1–42}$ t(13)=2.672 and p=0.0192; *App*$^{NL\text{-}G\text{-}F}$ soluble $A\beta_{1–42}$ t(13)=1.127 and p=0.2799; *App*$^{NL\text{-}G\text{-}F}$ insoluble $A\beta_{1–40}$ t(13)=2.644 and p=0.0203; *App*$^{NL\text{-}G\text{-}F}$ soluble $A\beta_{1–40}$ t(13)=1.294 and p=0.2182, mean ± SEM, n=8 animals).

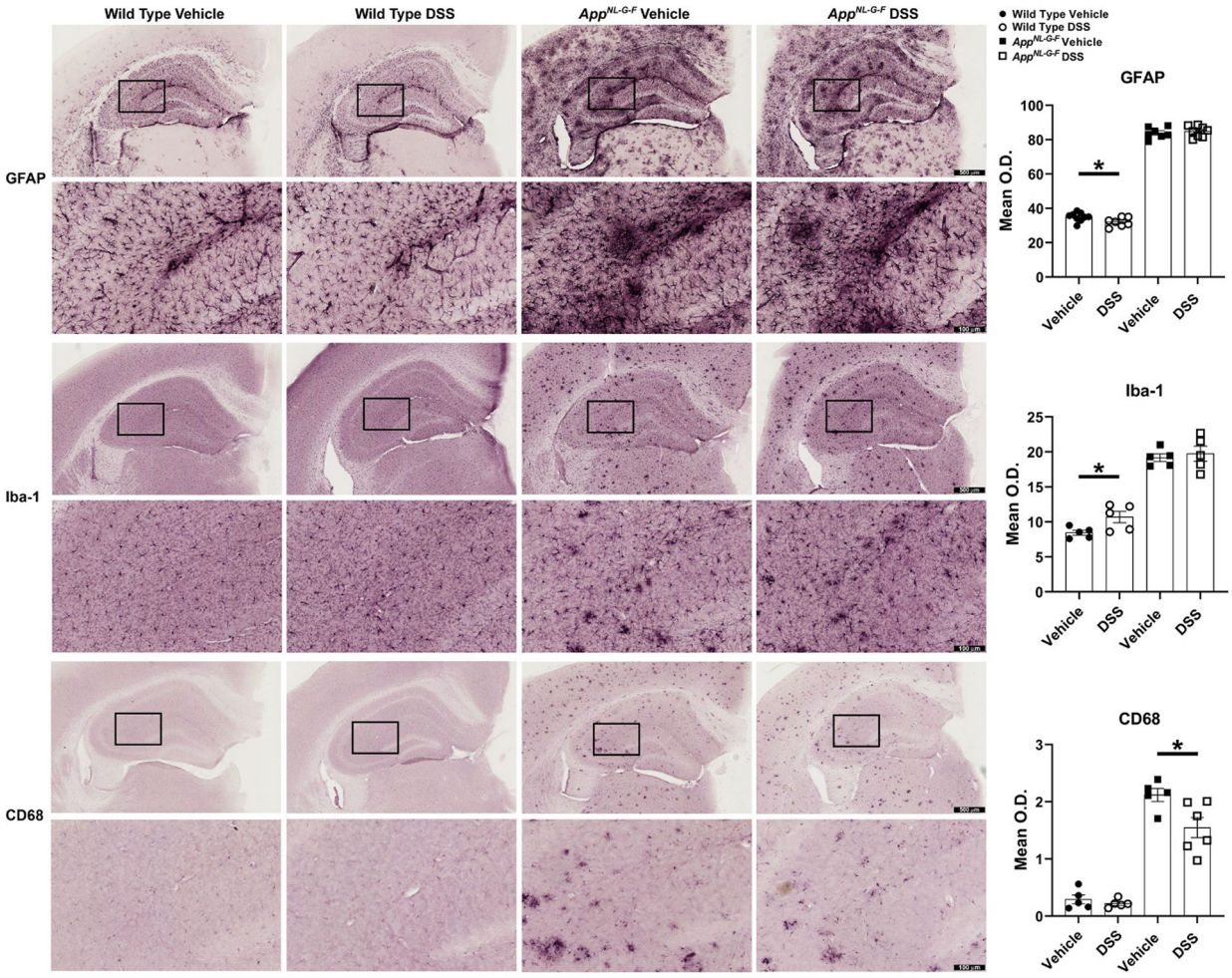

Fig. 7.

DSS treatment reduced microglia phagocytic phenotype in *App*$^{NL\text{-}G\text{-}F}$ mice but altered microgliosis and astrocytosis in wild types. Immunohistochemistry was performed on both WT and *App*$^{NL\text{-}G\text{-}F}$ brains using anti-GFAP, Iba-1, and CD68 antibodies. Mean optical density was measured using 3 hippocampal sections/mouse/condition. Representative hippocampi are shown with 4X and 20X magnifications, (*$p<0.05$, unpaired two-tailed t-test indicate WT GFAP $t(14)=2.289$ and $p=0.0381$; *App*$^{NL\text{-}G\text{-}F}$ GFAP $t(13)=0.4900$ and $p=0.6323$; WT Iba-1 $t(8)=2.533$ and $p=0.0351$; *App*$^{NL\text{-}G\text{-}F}$ Iba-1 $t(8)=0.4805$ and $p=0.6438$; WT CD68 $t(8)=0.8152$ and $p=0.4386$; *App*$^{NL\text{-}G\text{-}F}$ CD68 $t(9)=2.606$ and $p=0.0285$, mean ± SEM, n=5–9 animals).

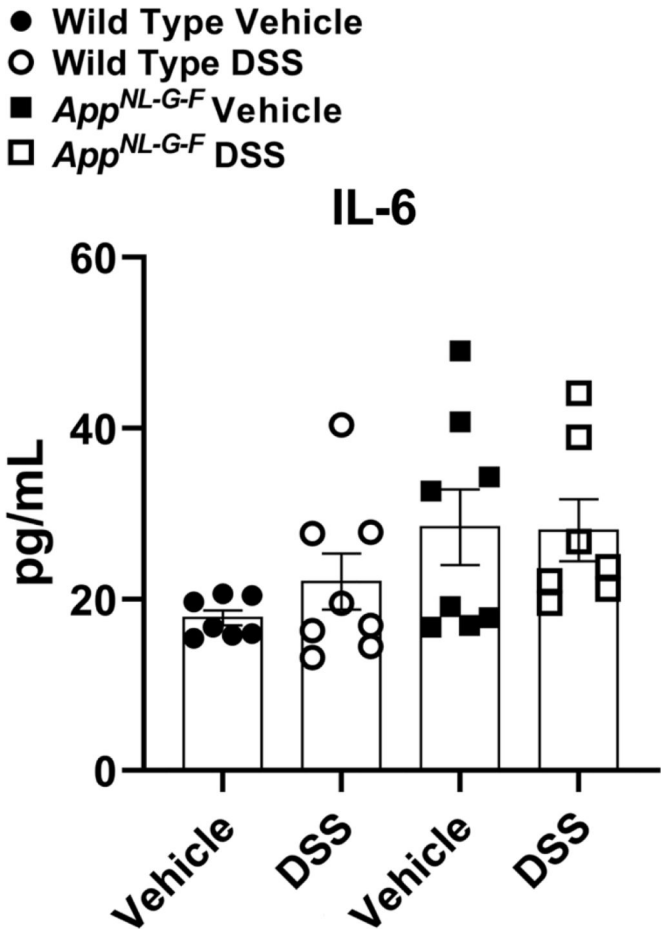

Fig. 8.

Brain IL-6 levels did not change due to DSS treatment. Parietal cortices collected from vehicle and DSS treated WT and *App*$^{NL\text{-}G\text{-}F}$ mice and were lysed to quantify the protein levels of IL-6 by ELISA, (unpaired two-tailed t-test indicate WT IL-6 t(13)=1.169 and p=0.2635; *App*$^{NL\text{-}G\text{-}F}$ IL-6 t(13)=0.06440 and p=0.9496, mean ± SEM, n=8 animals).

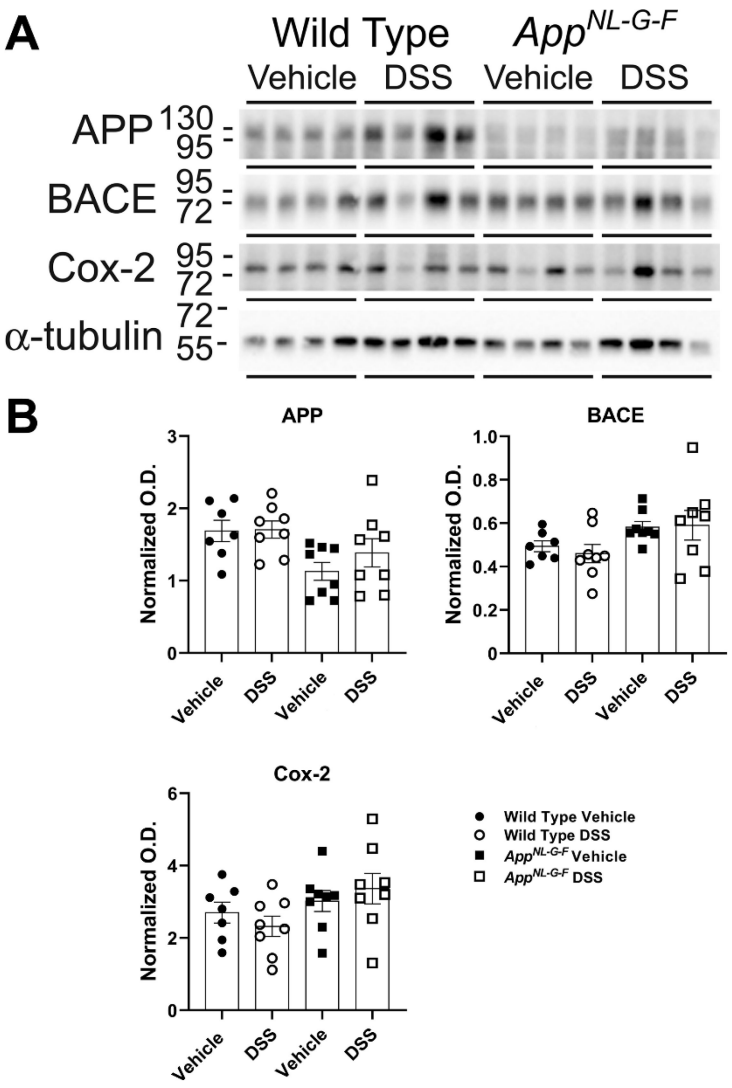

Fig. 9.

DSS treatment did not alter APP, BACE, and Cox-2 protein levels. **(A)** Hippocampal lysates from vehicle and DSS treated WT and *App*$^{NL\text{-}G\text{-}F}$ mice were western blotted to **(B)** quantify changes in APP, BACE, and Cox-2 levels using α-tubulin as the loading control, (unpaired two-tailed t-test indicate WT APP t(13)=0.09965 and p=0.9221; *App*$^{NL\text{-}G\text{-}F}$ APP t(14)=1.111 and p=0.2855; WT BACE t(13)=0.6603 and p=0.5206; *App*$^{NL\text{-}G\text{-}F}$ BACE t(14)=0.1222 and p=0.9045; WT Cox-2 t(13)=0.9480 and p=0.3604; *App*$^{NL\text{-}G\text{-}F}$ Cox-2 t(14)=0.6723 and p=0.5124; mean ± SEM, n=8 animals).

Table 1.

Animal numbers and age at beginning of the experiment.

Gender	Genotype	Age at the beginning of the Experiment	Genotype	Age at the beginning of the Experiment
Male	**Wild Type Vehicle (n=9)**	7–8 month-old	**Wild Type DSS (n=11)**	6–7 month-old
Male	***App*$^{NL-G-F}$ Vehicle (n=10)**	9–10 month-old	***App*$^{NL-G-F}$ DSS (n=10)**	10 month-old

Table 2.

Disease activity index (DAI) score performed to assess the colitis induced by DSS.

Score	Weight loss (%)	Stool consistency	Occult/gross bleeding
0	Wl < 1%	Normal	Normal
1	1% ≤ Wl < 5%		+
2	5% ≤ Wl < 10%	Loose stool	++
3	10% ≤ Wl < 20%		+++
4	Wl ≥ 20%	Diarrhea	Gross bleeding